

Doppler-Derived Renal Venous Stasis Index in the Prognosis of Right Heart Failure

Faeq Husain-Syed, MD; Horst-Walter Birk, MD; Claudio Ronco, MD; Tanja Schörmann, MD; Khodr Tello, MD; Manuel J. Richter, MD; Jochen Wilhelm, PhD; Natascha Sommer, PhD; Ewout Steyerberg, PhD; Pascal Bauer, MD; Hans-Dieter Walrath, MD; Werner Seeger, MD; Peter A. McCullough, MD, MPH; Henning Gall, PhD;* H. Ardeschir Ghofrani, MD*

Background—Persistent congestion with deteriorating renal function is an important cause of adverse outcomes in heart failure. We aimed to characterize new approaches to evaluate renal congestion using Doppler ultrasonography.

Methods and Results—We enrolled 205 patients with suspected or prediagnosed pulmonary hypertension (PH) undergoing right heart catheterization. Patients underwent renal Doppler ultrasonography and assessment of invasive cardiopulmonary hemodynamics, echocardiography, renal function, intra-abdominal pressure, and neurohormones and hydration status. Four spectral Doppler intrarenal venous flow patterns and a novel renal venous stasis index (RVSI) were defined. We evaluated PH-related morbidity using the Cox proportional hazards model for the composite end point of PH progression (hospitalization for worsening PH, lung transplantation, or PH-specific therapy escalation) and all-cause mortality for 1-year after discharge. The prognostic utility of RVSI and intrarenal venous flow patterns was compared using receiver operating characteristic curves. RVSI increased in a graded fashion across increasing severity of intrarenal venous flow patterns ($P < 0.0001$) and was significantly associated with right heart and renal function, intra-abdominal pressure, and neurohormonal and hydration status. During follow-up, the morbidity/mortality end point occurred in 91 patients and was independently predicted by RVSI (RVSI in the third tertile versus referent: hazard ratio: 4.72 [95% CI, 2.10–10.59; $P < 0.0001$]). Receiver operating characteristic curves suggested superiority of RVSI to individual intrarenal venous flow patterns in predicting outcome (areas under the curve: 0.789 and 0.761, respectively; $P = 0.038$).

Conclusions—We propose RVSI as a conceptually new and integrative Doppler index of renal congestion. RVSI provides additional prognostic information to stratify PH for the propensity to develop right heart failure.

Clinical Trial Registration—URL: <https://www.clinicaltrials.gov/>. Unique identifier: NCT03039959. (*J Am Heart Assoc.* 2019;8:e013584. DOI: 10.1161/JAHA.119.013584.)

Key Words: cardiorenal syndromes • intrarenal venous flow patterns • pulmonary hypertension • renal Doppler ultrasonography • venous congestion

Heart failure (HF) is a major cause of death worldwide¹ and the leading cause of hospitalization in both the United States and Europe.² In addition to low cardiac output,

persistent congestion with deterioration of renal function due to progressive right ventricular (RV) failure has been identified as an important cause of adverse outcomes in HF.^{3–5}

From the Division of Nephrology, Department of Internal Medicine II (F.H.-S., H.-W.B., T.S., W.S.), Division of Pulmonology and Critical Care Medicine, Department of Internal Medicine II (F.H.-S., K.T., M.J.R., N.S., H.-D.W., W.S., H.G., H.A.G.), and Department of Internal Medicine I, Division of Cardiology and Angiology (P.B.), University Hospital Giessen and Marburg, Giessen, Germany; International Renal Research Institute of Vicenza, Department of Nephrology, Dialysis and Transplantation, San Bortolo Hospital, Vicenza, Italy (F.H.-S., C.R.); Member of the German Centre for Lung Research (DZL), Universities of Giessen and Marburg Lung Centre (UGMLC), Giessen, Germany (K.T., M.J.R., J.W., N.S., H.-D.W., W.S., H.G., H.A.G.); Departments of Public Health (E.S.) and Epidemiology (H.G.), Erasmus MC, Rotterdam, The Netherlands; Department of Biomedical Data Sciences, Medical Statistics and Medical Decision Making, Leiden University Medical Center, Leiden, The Netherlands (E.S.); Max Planck Institute for Heart and Lung Research, Bad Nauheim, Germany (W.S.); Department of Pulmonology, Kerckhoff-Klinik, Nauheim, Germany (H.A.G.); Baylor Heart and Vascular Institute, Baylor University Medical Center at Dallas, TX (P.A.M.).

Accompanying Data S1, Tables S1 through S13, Figures S1 through S5 available at <https://www.ahajournals.org/doi/suppl/10.1161/JAHA.119.013584>

*Dr Gall and Dr Ghofrani are co-last authors.

Correspondence to: Faeq Husain-Syed, MD, University Hospital Giessen and Marburg, Department of Internal Medicine II, Division of Nephrology, Pulmonology and Critical Care Medicine, Klinikstrasse 33, 35392 Giessen, Germany. E-mail: faeq.husain-syed@innere.med.uni-giessen.de

Received June 13, 2019; accepted September 12, 2019.

© 2019 The Authors. Published on behalf of the American Heart Association, Inc., by Wiley. This is an open access article under the terms of the Creative Commons Attribution-NonCommercial-NoDerivs License, which permits use and distribution in any medium, provided the original work is properly cited, the use is non-commercial and no modifications or adaptations are made.

Clinical Perspective

What Is New?

- Doppler-derived intrarenal venous flow patterns having been shown to predict adverse outcomes in patients with heart failure; however, these approaches do not reflect the continuum of renal congestion because classification of intrarenal venous flow into different categories may miss important changes within those categories.
- In patients with suspected pulmonary hypertension undergoing right heart catheterization, we developed a continuous index from intrarenal venous flow patterns, and we propose the renal venous stasis index as a conceptually new and integrative Doppler measure of renal congestion.
- Our study suggests that renal venous stasis index may be superior to individual intrarenal venous flow pattern in predicting outcome in patients with pulmonary hypertension.

What Are the Clinical Implications?

- Renal venous stasis index provides additional prognostic information to stratify pulmonary hypertension for the propensity to develop right heart failure.
- Longitudinal studies are needed to clarify the role of renal venous stasis index in the management of pulmonary hypertension.

Congestion may lead to a vicious circle of renal dysfunction, increases in intra-abdominal pressure, neurohormonal activation, excessive renal tubular sodium reabsorption, fluid overload, and diuretic resistance, leading to further RV stress.^{6,7} Elevation of right atrial pressure (RAP) is transmitted to the renal veins, causing increased interstitial and tubular hydrostatic pressure within the encapsulated kidney, which decreases net glomerular filtration rate (GFR) and oxygen delivery.⁸ Similar pathophysiological mechanisms are expected to occur during increases in intra-abdominal pressure.⁶ Congestion may also directly compress vessels in the renal parenchymal regions or reduce vessel compliance.⁹ Consequently, changes in vessel shape and function may lead to transient and cardiac cycle-dependent stasis of renal venous flow and to changes in intrarenal venous flow (IRVF) patterns.

Doppler ultrasonography was recently proposed to evaluate renal congestion, with different IRVF patterns and the intrarenal venous impedance index having been shown to predict diuretic response and adverse outcomes in patients with HF or undergoing cardiac surgery.^{9–12} However, these approaches do not reflect the continuum of renal congestion: classification of IRVF patterns into different categories may miss important changes within those categories, and the

venous impedance index does not distinguish between IRVF patterns with different degrees of venous stasis. We sought to identify and rigorously characterize a new approach to evaluate the continuum of renal congestion based on Doppler renal venous flow.

Methods

Study Design and Participants

We prospectively enrolled consecutive hospital inpatients aged ≥ 18 years with suspected or prediagnosed pulmonary hypertension (PH) who were undergoing invasive right heart catheterization (RHC) between January 2017 and September 2017 at the Department of Pulmonology, University Hospital Giessen and Marburg, Giessen, Germany. PH is the most common precursor to RV failure¹³ and thus represents an ideal scenario for studying congestion. Suspicion of PH was determined on clinical grounds including echocardiographic evaluation, in accordance with the most recent guidelines for the diagnosis and treatment of PH.¹⁴ Patients with prediagnosed PH had received the diagnosis based on previous RHC. Diagnosis and classification of PH and pulmonary vasoactive treatment were based on current guidelines.¹⁴ PH was defined as invasively measured mean pulmonary arterial pressure (PAP) ≥ 25 mm Hg at rest. Patients were assigned a diagnosis of pulmonary arterial hypertension (group 1), PH due to left heart disease (group 2), PH due to lung diseases and/or hypoxia (group 3), chronic thromboembolic PH (group 4), or PH with unclear and/or multifactorial mechanisms (group 5)¹⁴ by a multidisciplinary board. Patients receiving PH therapy could enter the study without restrictions. HF was diagnosed according to current guidelines.¹⁵

Patients were excluded if they had chronic kidney disease stage 5, preexisting acute kidney injury, non-end-stage renal disease with extracorporeal or peritoneal ultrafiltration due to diuretic-resistant fluid overload, prediagnosed glomerulonephritis, autosomal dominant polycystic kidney disease, or postrenal obstruction; if they were recipients of solid-organ transplants; or if they had received NSAIDs within 72 hours before RHC. The exclusion criteria acute kidney injury and chronic kidney disease were diagnosed by an adjudication committee of 3 expert nephrologists. Chronic kidney disease was considered as estimated GFR (eGFR; creatinine–cystatin C equation) < 60 mL/min per 1.73 m^2 or the presence of microalbuminuria independent of eGFR.¹⁶ Acute kidney injury was defined as an increase in serum creatinine by ≥ 0.3 mg/dL within 48 hours or ≥ 1.5 times baseline within the prior 7 days¹⁷ (determined by all available serum creatinine values from hospital and outpatient medical records within the previous 90 days). Diuretic-resistant fluid overload was defined as the inability to achieve an adequate negative fluid

balance when the following 4 therapeutic options had been exploited: (1) restriction of fluid intake to <1.5 L/day and sodium chloride intake to ≤ 6.0 g/day; (2) (continuous) intravenous infusion of furosemide (minimum 500 mg/day); (3) sequential nephron blockade with the addition of a thiazide diuretic (eg, hydrochlorothiazide minimum 25 mg/day or xipamide minimum 20 mg/day); (4) addition of an aldosterone antagonist if tolerable with serum potassium level (spironolactone minimum 25 mg/day or eplerenone minimum 50 mg/day). RHC data, echocardiography, renal function, IRVF patterns, laboratory measurements, intra-abdominal pressure, and bioimpedance data were evaluated separately, as described in the next section, by examiners who were blinded to the other data. All patients were included in the Giessen PH registry.¹⁸

The study was approved by the local Human Research Ethics Committee (AZ 237/16) and complied with the Declaration of Helsinki. The study was registered at ClinicalTrials.gov (identifier: NCT03039959). All participants gave signed informed consent. The data that support the findings of this study are available from the corresponding author on reasonable request.

Procedures and Measurements

Renal Doppler ultrasonography

Ultrasound and spectral Doppler analyses were performed in duplicate by 2 independent nephrologists with experience in Doppler ultrasound, using an EPIQ 5 system (Philips Healthcare) with a sector transducer frequency range of 2.5–5.0 MHz. The analyses were performed after a Swan-Ganz catheter had been inserted for RHC assessment (described in the next section) and the patient had rested in a supine position for ≥ 10 minutes. Color Doppler images were used to identify interlobar vessels. Pulsed Doppler waveforms of the interlobar arteries and veins were recorded simultaneously with the patient in a resting decubitus position. Except for renal resistive index (RRI), which was assessed in both kidneys, all renal Doppler ultrasonography studies were performed in the right kidney (except in cases of unsatisfactory image quality) because left renal vein phasicity may be attenuated because of entrapment in the fork between the abdominal aorta and the superior mesenteric artery. In addition, the left ovarian or testicular veins drain into the left renal vein, which, in the rare event of ovarian or testicular varicosis, may affect renal venous flow.

All values were recorded as means of at least 3 measurements obtained in different interlobar vessels over 3 cardiac cycles during sinus rhythm. If atrial fibrillation was present, an index beat (the beat following 2 preceding cardiac cycles of equal duration) was used for each measurement. Venous impedance index and RRI were calculated as follows:

(maximum flow velocity—minimum diastolic flow velocity)/maximum flow velocity.⁹ A side-to-side difference in RRI of $>5\%$ between the kidneys was considered indicative for significant renal artery stenosis.¹⁹ RRI <0.7 was regarded as normal.²⁰

IRVF patterns were characterized by a blinded adjudication committee comprising a nephrologist, an angiologist, and a pulmonologist blinded to clinical, laboratory, and RHC data. If 2 reviewers disagreed, a third reviewer provided input and consensus was developed. The IRVF patterns were broadly categorized into continuous (noncongestive) and discontinuous (nadir velocity=0) flow patterns. We further classified the discontinuous IRVF patterns into 3 stages: pulsatile, biphasic (with venous peaks during systole and diastole), and monophasic (with venous peak during diastole; Figure 1).

To reflect the full continuum of renal congestion, we defined and evaluated a new, continuous ratio, the renal venous stasis index (RVSI). RVSI indicates the proportion of the cardiac cycle during which there is no renal venous outlet flow and is calculated as follows: (cardiac cycle time—venous flow time)/cardiac cycle time (Figure 2).

Right heart catheterization

On the day of RHC, each patient took his or her usual dose of medication at 07:00 AM except for the maintenance dose of diuretics. In patients with long-term oxygen treatment, oxygen was applied via nasal cannula at the previously prescribed flow rate. A Swan-Ganz catheter (7F balloon tipped; Baxter Healthcare) was inserted under local anesthesia in the right internal jugular vein. RHC was performed according to current guidelines,¹⁴ with assessment of mean PAP, RAP, pulmonary vascular resistance, pulmonary capillary wedge pressure, cardiac output (thermodilution method), cardiac index, mean arterial pressure, and mixed venous oxygen saturation immediately after renal ultrasonography (for details see Data S1).

Echocardiography

Echocardiography was performed by experienced echocardiographers 1 day before RHC using Vivid E9 and Vivid S5 systems (GE Healthcare). Right heart parameters (RV myocardial performance index [Tei index], tricuspid annular plane systolic excursion, systolic PAP, right atrial size, basal diameter of the right ventricle, inferior vena cava diameter, and systolic free wall myocardial velocity) and left heart parameters (left atrial and ventricular diameters and the ratio of mitral inflow velocity to lateral annular relaxation velocity [E/e']) were measured as recommended.²¹

Other measures

Body composition (including hydration status) was analyzed by bioimpedance spectroscopy using the body composition

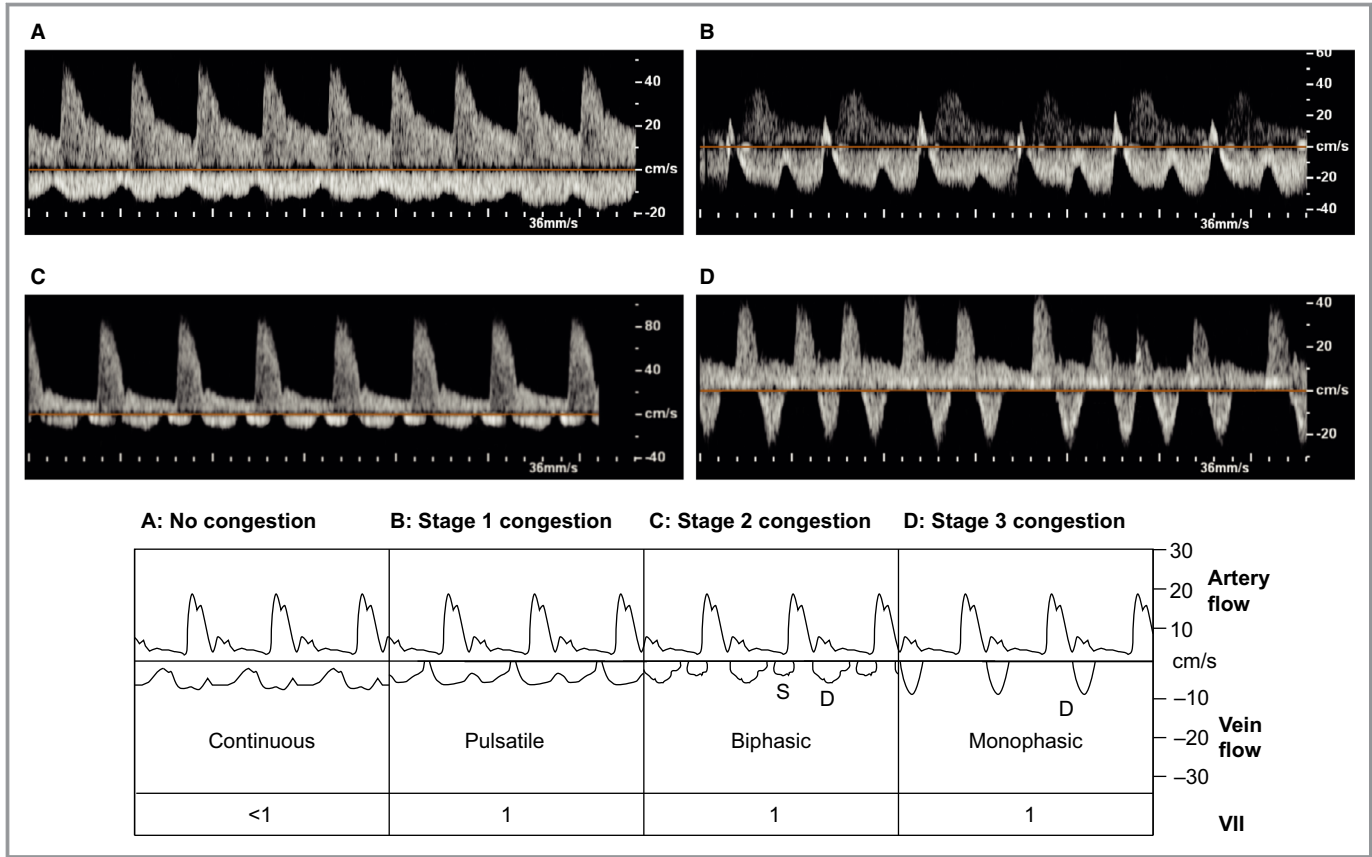


Figure 1. Congestion stages as defined by intrarenal venous flow patterns. Pulsed-wave Doppler samples of renal congestion patterns in the interlobar renal vessel. The upward Doppler signal shows the intrarenal arterial flow, which is used to measure renal resistive index; the downward Doppler signal shows the venous flow, used to measure venous impedance index or renal venous stasis index. **A**, No congestion: continuous venous flow. **B**, Stage 1 congestion: pulsatile venous flow. **C**, Stage 2 congestion: biphasic venous flow. **D**, Stage 3 congestion: monophasic venous flow. D indicates diastole; S, systole; VII, venous impedance index.

monitor (Fresenius Medical Care; see Data S1) before catheterization. Hydration status was also evaluated by clinical assessment (edema) and ultrasound (ascites and pleural effusion). Intra-abdominal pressure was measured via an indwelling urinary catheter in all patients using the transvesical method as previously described (Data S1).⁶ The mean arterial pressure was calculated as follows: [systolic blood pressure+(2×diastolic blood pressure)]/3. The abdominal perfusion pressure was determined as mean arterial pressure minus intra-abdominal pressure.⁶ The renal filtration gradient can be estimated as glomerular filtration pressure minus proximal tubular pressure.⁶ In the presence of elevated intra-abdominal pressure, proximal tubular pressure may be assumed to equal intra-abdominal pressure, and thus glomerular filtration pressure can be estimated mean arterial pressure minus intra-abdominal pressure. The renal filtration gradient was therefore calculated as follows: mean arterial pressure–(2×intra-abdominal pressure). Intra-abdominal pressures from 4 to 7 mm Hg were considered as normal range, whereas values ≥12 mm Hg were considered as intra-

abdominal hypertension.²² Six-minute walk distance and New York Heart Association functional class were assessed 1 day before RHC according to current guidelines.^{15,23} Loop diuretic doses were converted to furosemide equivalents with 20 mg torasemide equal to 80 mg furosemide for oral diuretics and 20 mg torasemide equal to 40 mg furosemide for intravenous diuretics.²⁴ Thiazide diuretics included hydrochlorothiazide and xipamide. If triamterene was taken, it was used in a fixed diuretic combination with hydrochlorothiazide. Aldosterone antagonists included spironolactone and eplerenone.

Laboratory methods

Laboratory methods are detailed in Data S1. Briefly, blood samples were collected on the day of RHC from the Swan-Ganz catheter after the patient had rested in a supine position for ≥60 minutes. Urine samples were collected from first morning-void specimens. BNP (B-type natriuretic peptide), copeptin, creatinine, and cystatin C were measured using chemiluminescence, time-resolved amplified cryptate emission, photometric-enzymatic, and immunoturbidimetric

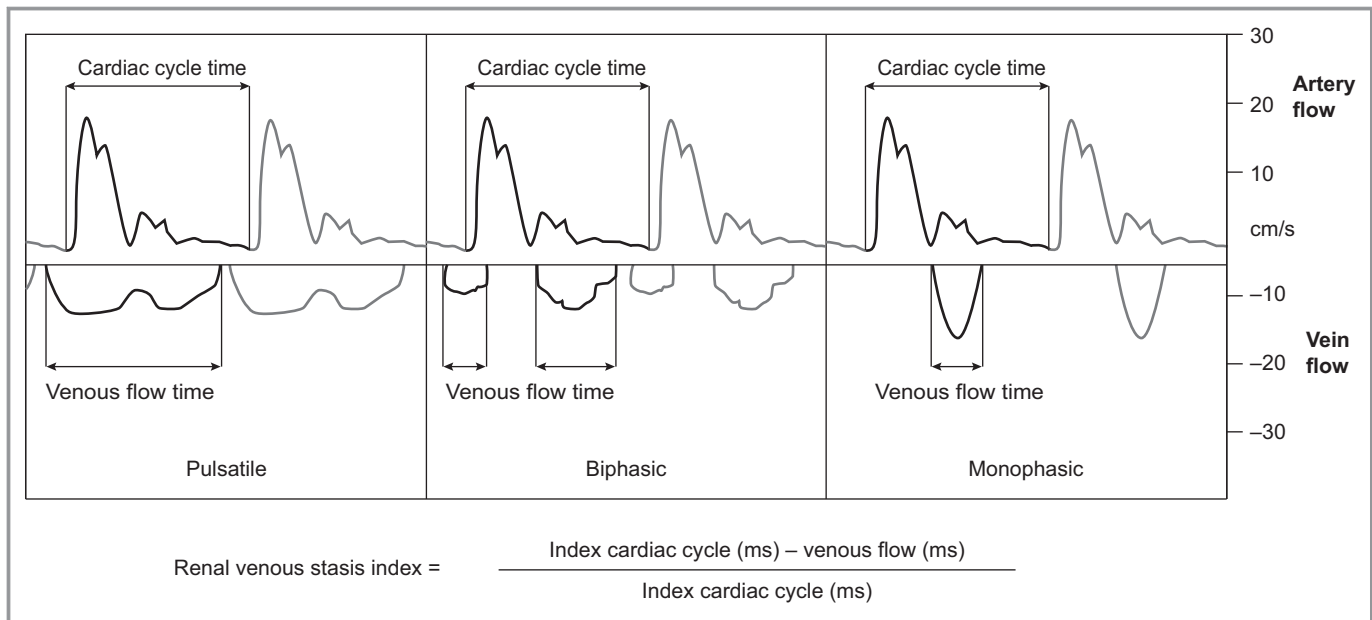


Figure 2. Renal venous stasis index (RVSI). The RVSI is a novel Doppler-based parameter to estimate severity of renal congestion. Pulsed-wave Doppler samples of renal congestion patterns in the interlobar renal vessel are shown. The upward Doppler signal shows the intrarenal arterial flow, which is used to measure cardiac cycle time; the downward Doppler signal shows the venous flow, used to measure venous flow time. Under physiological conditions, the index is zero due to the presence of a continuous venous flow, whereas it increases with rising severity of congestion. The figure illustrates the method of measurement of RVSI in different congestion stages. ms indicates milliseconds.

methods, respectively. We chose BNP and copeptin as biomarkers of neurohormonal activation because both are commonly used for diagnosis and determining prognosis in HF.¹⁵ The eGFR was determined using both creatinine²⁵ and creatinine–cystatin C²⁶ Chronic Kidney Disease–Epidemiology Collaboration equations.

Follow-Up and End Points

Clinical outcomes were evaluated for 1 year after discharge. Patients were closely followed during the observation period by clinical visits or telephone interviews. Changes of medication for clinical reasons were permitted (the primary physician caring for the patient was blinded to the IRVF patterns and RVSI results). Use of diuretics was at the discretion of the treating physician. At 1 year, all patients were recontacted for follow-up analyses at the nephrology outpatient department. If the primary cause of PH was surgically treated (eg, pulmonary thromboendarterectomy in patients with chronic thromboembolic PH or lung transplantation), the patients were followed until the surgical procedure. If a patient died outside of the hospital, telephone calls to the general practitioner or the family members were performed to confirm the date of death.

We evaluated the first occurrence of a composite end point of PH-related morbidity (any hospitalization for worsening of PH, lung transplantation, or need for escalation of PH-specific

therapy) and death from any cause. In addition, the following components of the composite end point were each analyzed separately: unscheduled hospitalization due to fluid overload with requirement for an increase in diuretic therapy (eg, due to pulmonary or peripheral edema, pleural effusion, ascites, or recent increase of body weight by $\geq 10\%$); need for escalation or change of PH-specific therapy due to clinical and echocardiographic progress of PH; and death from any cause. Patients who underwent pulmonary thromboendarterectomy were considered as withdrawn alive. All available medical records were collected, and morbidity and mortality data were evaluated according to the predefined end point components in a blinded fashion by a clinical end point adjudication committee including medical experts in nephrology, PH, and cardiology who were unaware of the IRVF patterns and RVSI results and not responsible for the primary care of the patient.

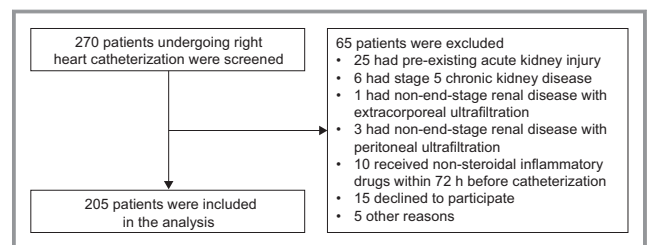


Figure 3. Study flow chart. The diagram describes the protocol used for the enrollment of patients in this study.

Table 1. Clinical Characteristics, Invasive Hemodynamics, Echocardiographic Data, Renal Function, and Neurohormonal and Hydration Status According to RVSI Tertile

	All patients(N=205)	RVSI 0(n=59)	RVSI Tertiles			P Value*
			First, 0 to ≤0.12 (n=49)	Second, >0.12 to ≤0.32 (n=48)	Third, >0.32(n=49)	
Demographics						
Age, y	68.0 (57.0–78.0)	68.0 (55.0–73.0)	67.0 (51.0–75.5)	72.5 (61.0–78.0)	74.0 (65.0–81.0)	0.0152
Male, n (%)	87 (42.4)	24 (40.7)	17 (34.7)	17 (35.4)	29 (59.2)	0.0488
Body mass index, kg/m ²	27.82±6.07	29.03±6.05	26.05±6.37	28.30±6.84	27.67±4.52	0.075
Baseline clinical data						
Oxygen supply, n (%)	118 (57.6)	28 (47.5)	28 (57.1)	32 (66.7)	30 (61.2)	0.224
Pao ₂ [†]	69.32±11.71	71.09±10.74	68.11±11.21	68.00±10.01	69.67±14.57	0.474
PacO ₂ [†]	38.57±8.98	40.20±11.68	37.76±7.30	37.38±7.88	38.59±7.66	0.367
6MWD, m	277.23±136.05	309.76±118.16	285.08±156.43	283.77±131.30	223.80±127.02	0.0098
NYHA classification, n (%)						
1–2	44 (21.5)	15 (25.4)	12 (24.5)	13 (27.1)	4 (8.2)	0.178
3–4	161 (78.5)	44 (74.6)	37 (75.5)	35 (72.9)	45 (91.8)	
Laboratory data						
Leukocytes, ×10 ⁹ /L	7.43±2.49	7.33±2.53	7.72±2.29	7.14±2.68	7.56±2.47	0.674
Hemoglobin, g/dL	13.27±2.09	13.95±1.83	13.53±2.06	13.49±2.18	13.02±2.31	0.504
Sodium, mmol/L	139.56±3.07	139.32±3.15	139.73±2.72	140.15±3.14	139.10±3.22	0.343
Potassium, mmol/L	3.67±0.42	3.65±0.40	3.64±0.34	3.63±0.44	3.73±0.47	0.612
Uric acid, mg/dL	6.77±2.52	6.26±2.18	5.89±2.07	6.65±2.31	8.38±2.82	<0.0001
Albumin, g/dL	38.20±3.22	38.91±3.18	37.49±3.25	38.09±2.96	38.18±2.42	0.162
C-reactive protein, mg/L	5.22 (1.52–11.44)	3.13 (1.07–8.60)	3.70 (0.50–11.58)	5.22 (2.05–11.48)	7.20 (3.18–14.51)	0.0172
Comorbidities, n (%)						
Hypertension	128 (62.4)	35 (59.3)	29 (59.2)	32 (66.7)	32 (65.3)	0.800
Diabetes mellitus	48 (23.4)	12 (20.3)	9 (18.4)	9 (18.8)	18 (36.7)	0.092
Atrial fibrillation	56 (27.3)	7 (11.9)	14 (28.6)	9 (18.8)	26 (53.1)	<0.0001
Maintenance therapy						
ACEI or ARB, n (%)	83 (40.5)	23 (39.0)	18 (36.7)	20 (41.7)	22 (44.9)	0.858
β-Blocker	103 (50.2)	25 (42.4)	18 (36.7)	27 (56.3)	33 (67.3)	0.0095
Loop diuretic dose, mg/d [‡]	40 (0.0–60.0)	20 (0.0–40.0)	20 (0.0–55.0)	30 (0.0–55.0)	80 (40.0–170.0)	<0.0001
PH-specific therapy (%)						
Treatment-naïve	116 (56.6)	42 (71.2)	21 (42.9)	25 (47.9)	30 (61.2)	0.0292
Monotherapy	49 (23.9)	8 (13.6)	18 (36.7)	11 (22.9)	12 (24.5)	
Dual therapy	28 (13.7)	6 (10.2)	7 (14.3)	12 (25.0)	3 (6.1)	
Triple therapy	12 (5.9)	3 (5.1)	3 (6.1)	2 (4.2)	4 (8.2)	
Hemodynamics						
Mean PAP, mm Hg	34.84±14.63	24.10±9.62	34.78±12.79	41.10±16.03	41.69±12.39	<0.0001
PVR, dyne·s/cm ⁵	394 (214–604)	229 (110–420)	422 (214–589)	516 (279–679)	495 (313–833)	<0.0001
RAP, mm Hg	5.76±5.63	2.46±3.66	3.88±3.76	5.56±3.72	11.80±6.06	<0.0001
Cardiac index, L/min/m ²	2.73±0.98	2.98±1.01	2.88±1.16	2.67±0.68	2.32±0.89	0.0032
PCWP, mm Hg	9.0 (5.0–13.0)	7.0 (4.0–10.0)	8.0 (5.0–12.0)	9.5 (6.0–14.8)	12.0 (8.0–18.0)	<0.0001

Continued

Table 1. Continued

	All patients(N=205)	RVSI 0(n=59)	RVSI Tertiles			P Value*
			First, 0 to ≤0.12 (n=49)	Second, >0.12 to ≤0.32 (n=48)	Third, >0.32(n=49)	
Mixed venous oxygen saturation, %	63.76±8.35	66.70±6.42	65.15±7.17	65.00±5.85	57.62±10.43	<0.0001
Heart rate, beats/min	71.62±13.23	72.00±11.32	69.84±12.90	71.38±11.49	73.18±16.95	0.65
MAP, mm Hg [§]	84.25±11.57	85.22±10.28	82.76±13.39	84.81±10.82	84.02±11.99	0.72
Echocardiographic parameters						
Right heart						
TAPSE, mm	19.89±4.41	21.88±3.82	21.14±4.44	19.50±3.64	16.63±3.85	<0.0001
RV myocardial performance index (Tei index)	0.49±0.22	0.46±0.20	0.45±0.21	0.54±0.24	0.49±0.24	0.334
RV S', cm/s	11.60±3.52	12.95±3.31	12.13±3.27	11.49±3.29	9.54±3.36	<0.0001
TAPSE/systolic PAP ratio	0.39±0.21	0.55±0.24	0.38±0.22	0.33±0.12	0.30±0.12	<0.0001
Tricuspid insufficiency, n (%)						<0.0001
Mild	66 (32.2)	34 (57.6)	10 (20.4)	12 (25.0)	10 (20.4)	
Moderate	112 (54.6)	23 (39.0)	31 (63.3)	32 (66.7)	26 (53.1)	
Severe	25 (12.2)	1 (1.7)	7 (14.3)	4 (8.3)	13 (26.5)	
RA area, cm ²	18.89±6.72	15.14±6.30	18.48±5.64	19.21±5.64	23.58±6.44	<0.0001
RV diameter, mm	40.78±8.08	37.93±7.38	41.09±6.97	40.52±7.75	44.40±9.00	0.0005
IVC, cm	2.27±0.49	2.01±0.52	2.26±0.42	2.34±0.41	2.53±0.43	<0.0001
Left heart						
LVEF, %	60.0 (60.0–65.0)	60 (60.0–65.0)	62 (60.0–65.0)	60 (60.0–65.0)	60 (55.0–65.0)	0.0442
LA diameter, mm	41.98±6.86	39.78±6.35	40.33±6.98	41.42±6.16	46.43±5.98	<0.0001
LVEDD, mm	46.03±5.59	46.28±4.73	45.26±5.73	45.83±6.23	46.67±5.81	0.65
E/e' ratio	12.98±5.34	11.07±3.52	12.46±4.50	14.09±5.69	14.79±6.78	0.0023
Renal function						
Serum creatinine, mg/dL	1.01±0.45	0.92±0.40	0.79±0.21	0.98±0.36	1.35±0.55	<0.0001
Cystatin C, mg/L	1.10 (0.91–1.52)	0.98 (0.81–1.24)	1.01 (0.88–1.18)	1.27 (0.97–1.62)	1.53 (1.10–2.09)	<0.0001
Urea, mg/dL [¶]	47.44±35.85	40.97±26.71	34.29±13.13	44.69±25.25	71.10±54.75	<0.0001
eGFR (CKD-EPI creatinine equation), mL/min/1.73 m ² #	74.45±26.12	80.07±24.52	87.31±18.86	72.69±24.01	56.57±26.75	<0.0001
eGFR (CKD-EPI creatinine–cystatin C equation), mL/min/1.73 m ² **	68.58±26.86	77.68±27.65	80.80±20.25	64.06±22.56	49.84±24.49	<0.0001
Renal filtration gradient, mm Hg ^{††}	69.30±12.46	73.70±10.60	69.62±13.32	69.81±11.12	63.20±12.81	<0.0001
Urine PCR, mg/g creatinine	58.8 (40.2–114.2)	51.5 (36.4–72.6)	55.3 (37.5–85.4)	58.0 (39.9–92.9)	116.2 (49.1–190.8)	<0.0001
Urine ACR, mg/g creatinine	11.4 (6.3–29.7)	9.3 (5.2–16.0)	9.0 (5.7–18.5)	10.3 (6.7–19.0)	29.7 (11.7–107.8)	<0.0001
Urine α1MCR, mg/g creatinine	10.9 (6.0–19.1)	8.7 (5.1–16.5)	8.7 (5.7–15.1)	12.0 (6.5–21.4)	15.4 (7.6–32.7)	0.0092
Renal Doppler ultrasonography						
Venous impedance index	0.84±0.26	0.44±0.12	1.00±0	1.00±0	1.00±0	<0.0001
RRI	0.71±0.07	0.69±0.08	0.69±0.07	0.73±0.07	0.74±0.06	<0.0001

Continued

Table 1. Continued

	All patients(N=205)	RVSI 0(n=59)	RVSI Tertiles			P Value*
			First, 0 to ≤0.12 (n=49)	Second, >0.12 to ≤0.32 (n=48)	Third, >0.32(n=49)	
Neurohormonal status						
BNP, pg/mL	138.0 (50.0–321.0)	46.0 (26.0–113.0)	98.0 (38.0–264.5)	198.5 (111.3–322.5)	468.0 (228.5–820.0)	<0.0001
Copeptin, pmol/L	11.1 (5.8–23.3)	9.1 (4.6–16.0)	7.3 (4.9–14.4)	14.0 (5.2–23.5)	23.2 (11.1–39.6)	<0.0001
Urine feNa, %	0.6 (0.4–1.3)	0.7 (0.4–1.2)	0.6 (0.4–1.1)	0.6 (0.4–1.2)	1.2 (0.4–2.1)	0.072
Hydration status						
Peripheral edema, n (%)	60 (29.3)	13 (22.0)	11 (22.4)	16 (33.3)	20 (40.8)	0.105
Pleural effusion, n (%)	17 (8.3)	3 (5.1)	3 (6.1)	3 (6.3)	8 (16.3)	0.137
Ascites, n (%)	7 (3.4)	0 (0)	1 (2.0)	0 (0)	6 (12.2)	0.0013
Hydration status (as measured by bioimpedance) ^{**}	0.71±2.12	−0.14±1.41	0.50±1.78	1.18±2.41	1.50±2.48	<0.0001
ECW/ICW ratio ^{**}	0.88±0.12	0.85±0.11	0.85±0.09	0.89±0.13	0.91±0.13	0.0286
Intra-abdominal pressure measurement						
Intra-abdominal pressure, mm Hg	7.0 (6.0–9.0)	6.0 (5.0–6.0)	6.0 (6.0–7.0)	7.0 (7.0–8.0)	10.0 (9.0–12.0)	<0.0001
Abdominal perfusion pressure, mm Hg ^{§§}	76.78±11.81	79.46±10.38	77.31±10.89	76.19±13.32	73.61±12.21	0.078

Values are mean±SD or median (interquartile range) except as noted. Additional data are provided in the Data S1. ACEI indicates angiotensin-converting enzyme inhibitor; ACR, albumin/creatinine ratio; α 1MCR, α 1-microglobulin/creatinine ratio; ARB, angiotensin receptor blocker; BNP, B-type natriuretic peptide; CKD-EPI, Chronic Kidney Disease Epidemiology Collaboration; ECW, extracellular water; E/e' ratio, ratio of mitral inflow velocity to lateral annular relaxation velocity; eGFR, estimated glomerular filtration rate; feNa, fractional excretion of sodium; ICW, intracellular water; IVC, inferior vena cava; LA, left atrial; LVEDD, left ventricular end-diastolic diameter; LVEF, left ventricular ejection fraction; MAP, mean arterial pressure; NYHA, New York Heart Association; PAP, pulmonary arterial pressure; PCR, protein/creatinine ratio; PCWP, pulmonary capillary wedge pressure; PH, pulmonary hypertension; PVR, pulmonary vascular resistance; RA, right atrial; RAP, right atrial pressure; RRI, renal resistive index; RV, right ventricular; RV S', systolic annular tissue velocity of the lateral tricuspid annulus; RVSI, renal venous stasis index; 6MWD indicates 6-min walk distance; TAPSE, tricuspid annular plane systolic excursion.

*After application of the Bonferroni correction, $P<0.0008$ was considered significant.

[†]Blood gas measurements were taken from arterialized capillary ear lobe blood during right heart catheterization. In patients with long-term oxygen treatment, oxygen was applied by nasal cannula at the previously prescribed flow rate. To convert mm Hg to kPa, multiply by 0.133.

[‡]A total of 14 patients received intravenous furosemide.

[§]MAP was calculated as follows: (systolic blood pressure+[2×diastolic pressure])/3.

^{||}To convert the values for serum creatinine to μ mol/L, multiply by 88.4.

[¶]To convert the values for urea to blood urea nitrogen, multiply by 0.467.

[#]eGFR was calculated with the CKD-EPI equation based on serum creatinine.²⁵

^{**}eGFR was calculated with the CKD-EPI equation based on serum creatinine and cystatin C.²⁶

^{††}The renal filtration gradient was calculated as follows: MAP−(2×intra-abdominal pressure).⁶

^{‡‡}Additional bioimpedance data are provided in Data S1.

^{§§}Abdominal perfusion pressure was calculated as MAP minus intra-abdominal pressure.⁶

Statistical Analysis

Descriptive statistics were expressed as mean±SD or median (interquartile range [IQR]) for continuous variables, and frequency (percentage) for categorical variables. Patient characteristics were compared between subgroups using ANOVA, Mann-Whitney U tests, or Kruskal–Wallis tests for continuous variables and χ^2 tests for categorical variables. Intra- and interobserver reliability was evaluated using the intraclass correlation coefficient. To understand the relationships of renal function and RVSI with other continuous variables, we performed Spearman and Pearson correlation analysis. Correlation coefficient values >0.3 were considered relevant. Kaplan–Meier analysis was performed to determine the

relationship of RVSI and IRVF patterns with clinical end points. Risk factors for clinical end points were determined with Cox proportional hazards models. Univariate factors with $P<0.05$ were entered into the multiple Cox regression model. A stepwise backward procedure was used in multiple Cox regression analysis (likelihood ratio). RVSI values >0 were divided into tertiles, and then the hazard rates of each tertile for reaching the clinical end points were calculated in relation to the control group (RVSI=0). Receiver operating characteristic curves were used to evaluate RVSI and IRVF as predictors of binary clinical end points. Time-to-event information and censoring were ignored when computing the areas under the curves. Receiver operating characteristics were compared with the DeLong test implemented in the R package pROC

(1.14.0).^{27,28} Overall, the significance level was set at $\alpha=0.05$ except in multiple Cox regression analysis, where the significance level was $\alpha=0.10$. The Bonferroni correction was applied to adjust for multiple testing. The size of the RHC cohort was estimated based on feasibility considerations. The power to detect a hazard ratio >2.0 at $\alpha=0.05$ between the third tertile RVSI group ($n=49$) versus RVSI=0 ($n=59$) was 50%. The power was calculated in R (3.5.1) using the function *powerCT* from the package *powerSurvEpi* (0.1.0), based on a method proposed by Freedman.^{27,29,30} All other statistical analyses were performed using SPSS 23.0 software (IBM Corp).

Results

Patients

Of 270 eligible patients undergoing RHC, 205 patients were enrolled and included in the analysis (Figure 3). None were lost to follow-up. In all patients except 2, renal Doppler studies were performed in the right kidney. IRVF pattern classifications were completely consistent, and RVSI measurements showed excellent reliability in both intra- and interobserver comparisons (Table S1). Patients' baseline characteristics are shown in Table 1 and Table S2.

Association of RVSI with IRVF patterns and demographic and clinical characteristics

After completion of recruitment, we confirmed the predefined IRVF patterns with invasive hemodynamics and echocardiography and assessed their associations with other parameters (Figure S1 and Table S3). By definition, patients with no renal

congestion had RVSI=0 and were assigned as the referent group. As shown, RVSI showed a significant stepwise increase along the predefined IRVF patterns ($P<0.0001$; Figure 4).

Table 1 and Figure 5 show the associations of RVSI tertiles with key clinical parameters (additional parameters are shown in Table S4). Cardiopulmonary hemodynamics (evaluated by RHC) worsened with increasing RVSI tertile, with RAP showing the clearest association. RV systolic function (tricuspid annular plane systolic excursion) showed a significant stepwise decrease along the tertiles, with manifest dysfunction at the highest tertile. Right atrial and ventricular diameter, left atrial diameter, and E/e' ratio significantly increased along the RVSI tertiles.

Patients with no congestion had normal mean serum creatinine and eGFR values. From the second RVSI tertile onward, there was gradual lower eGFR and renal filtration gradient across RVSI tertiles, whereas from RVSI=0 (no congestion) to the first RVSI tertile, there was no significant change in serum creatinine ($P=0.09$), eGFR ($P=0.53$), and cystatin C ($P=0.70$). RRI significantly increased with increasing RVSI tertile. Of note, none of the patients exhibited a significant difference in mean RRI values between kidneys (indicative of renal artery stenosis). There was a significant increase in proteinuria, albuminuria, and tubular proteinuria ($\alpha 1$ -microglobulin) with increasing RVSI tertile, but the median values stayed within the physiological range.

RVSI tertiles were associated with levels of BNP and copeptin, as well as hydration status (as measured by bioimpedance), loop diuretic dose, and intra-abdominal pressure. Fluid overload was detected as an extracellular fluid expansion in relation to intracellular fluid depletion. Of note, all patients with ascites were in the highest RVSI tertile and exhibited a monophasic IRVF pattern except 1 patient who was diagnosed with hepatitis C-associated liver cirrhosis and porto-PH who was within the first RVSI tertile.

Correlation analyses (Figure S2 and Table S5) showed relevant and statistically significant relationships between RVSI and cardiopulmonary hemodynamics, echocardiographic parameters, renal function, intra-abdominal pressure, and neurohormonal and hydration status. As expected, tricuspid insufficiency had an impact on RVSI values (median RVSI: 0.00 [IQR: 0.15–0.36] in mild, 0.13 [IQR: 0.17–0.46] in moderate, and 0.33 [IQR: 0.26–0.72] in severe tricuspid insufficiency; $P<0.0001$). However, in multivariate Cox regression analysis, RVSI was superior to tricuspid insufficiency in predicting the composite end point and all individual components. Furthermore, RVSI values were significantly increased in patients with versus without atrial fibrillation (0.28 versus 0.09; $P<0.0001$); this large difference was not due to interobserver variability (intraclass correlation coefficient was >0.9 in both groups).

Of the echocardiographic and hemodynamic parameters assessed, right atrial area and RAP showed the strongest

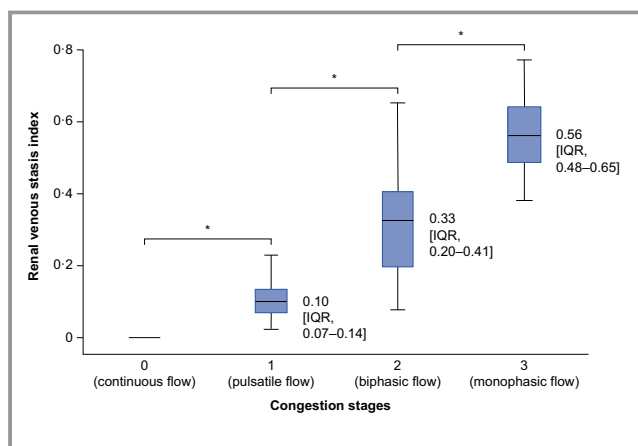


Figure 4. Association of renal venous stasis index with congestion stages. Under physiological conditions, the renal venous stasis index is zero due to the presence of a continuous venous flow, whereas it increases with rising severity of congestion. Horizontal lines indicate median, boxes indicate interquartile range (IQR), and whiskers indicate minimum and maximum values. Data labels show median (IQR).

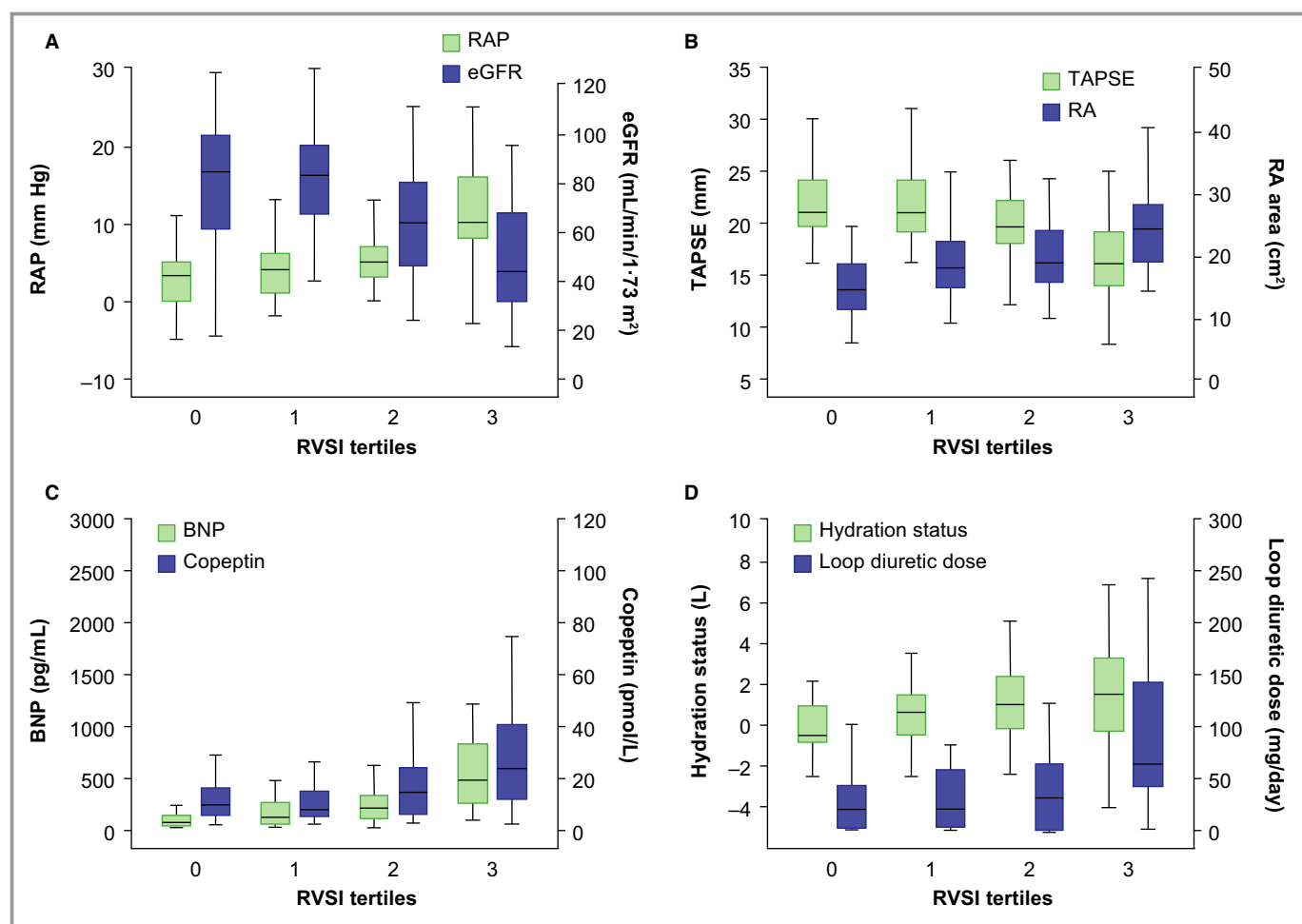


Figure 5. RVSI and associated clinical parameters. Severity of renal congestion can be evaluated by measurement of RVSI using renal Doppler ultrasonography. The figure illustrates the associations of RVSI tertiles with RAP and renal function (A), right ventricular systolic function and RA area (B), neurohormonal status (C), and hydration status (D). Fluid overload as measured by bioimpedance is likely to occur because of hemodynamic alterations and neurohormonal activation leading to a deterioration of renal function and fluid retention. BNP indicates B-type natriuretic peptide; eGFR, estimated glomerular filtration rate (based on Chronic Kidney Disease Epidemiology Collaboration creatinine–cystatin C equation); RA, right atrial; RAP, right atrial pressure; RVSI, renal venous stasis index; TAPSE, tricuspid annular plane systolic excursion; VII, venous impedance index.

correlations with renal function (Table S6). Arterial blood gas measurements showed no correlation with renal function.

Analysis of PH subtypes

Baseline parameters significantly differed across the PH subtype groups, and confirmed the correctness of the classification of each group (Table S7). All 30 patients with PH due to left heart disease had HF with preserved ejection fraction (Table S2). Patients with PH due to left heart disease exhibited the highest RVSI values and were most likely to have a monophasic pattern; they also had the poorest right and left heart function, lowest renal function, and highest BNP levels and intra-abdominal pressures.

Clinical outcomes

All 205 patients were included in the analysis of outcomes. During the observational period (12 months [range: 11–13

months]), the composite end point of PH-related morbidity and death from any cause occurred in 91 of 205 patients (Table S8). We observed 64 (31.2%) unscheduled hospitalizations for fluid overload, 71 (34.6%) escalations of PH-specific therapy, and 21 (10.2%) deaths. Five patients underwent pulmonary thromboendarterectomy, and 1 patient underwent lung transplantation.

Patients in higher RVSI tertiles had increased rates of the composite end point (Figure 6) and 2 of the individual components (Figure S3). Analysis of outcomes by IRVF patterns showed broadly similar trends but with some overlap between the groups with biphasic and monophasic IRVF patterns (Figure S4). In multiple Cox regression analysis, RVSI tertiles remained independent predictors of the composite end point and 2 of the individual components (Table 2; univariate analyses are provided in Tables S9–S12).

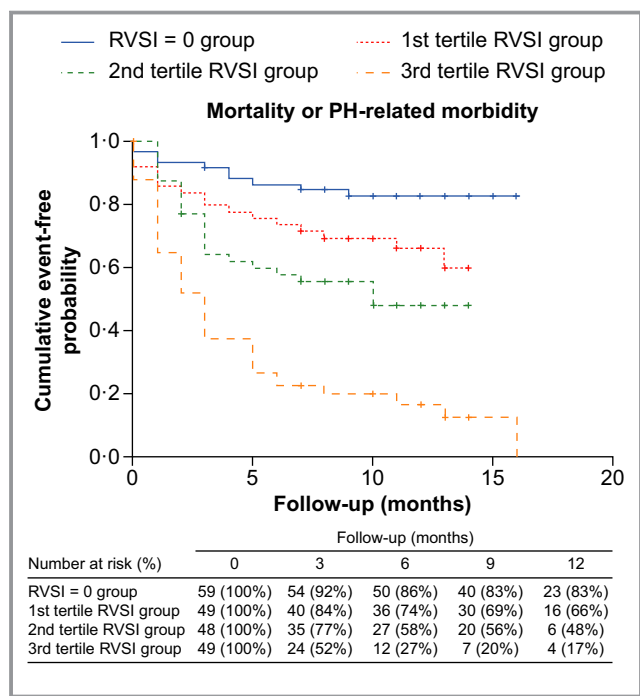


Figure 6. Kaplan-Meier estimate curve according to RVSI tertiles. Patients in the third tertile group had a significantly higher probability than other patients of the composite end point of PH-related morbidity or death from any cause ($P<0.0001$). PH indicates pulmonary hypertension; RVSI, renal venous stasis index.

During the observational period, 3 patients developed stage 3 acute kidney injury with diuretic-resistant fluid overload and required RRT; all 3 exhibited a monophasic IRVF pattern with a median RVSI of 0.64 (IQR: 0.59–0.73) at baseline.

RVSI versus IRVF patterns for prediction of clinical outcomes

Receiver operating characteristic curves suggested that RVSI was a more sensitive and specific predictor of the composite end point than the individual IRVF patterns (areas under the curve: 0.789 and 0.761, respectively; $P=0.038$; Figure S5). The maximal Youden statistic was obtained for an RVSI cutoff of 0.14, yielding 77% specificity and 63% sensitivity. $RVSI \geq 0.14$ was also an independent predictor of the composite end point when added in multiple Cox regression analysis instead of RVSI tertiles. A model including both RVSI and IRVF patterns as predictor variables indicated superiority of RVSI over IRVF patterns (Wald values: 2.817 and 2.059, respectively). Comparisons of RVSI and IRVF patterns for prediction of the individual component end points are shown in Figure S5 and Table S13.

Discussion

We developed a continuous index from Doppler-derived IRVF patterns and propose the RVSI as a simple, noninvasive, and

integrative Doppler measure of renal congestion. In patients undergoing RHC based on clinical grounds, the RVSI was correlated with invasive hemodynamics. Furthermore, our data suggest that the RVSI may be superior to individual IRVF patterns in predicting outcome.

Elevated RAP has been identified as a main driver of deteriorating renal function in acutely decompensated HF.^{3–5} Only 3 HF studies^{9–11} have previously investigated the association of Doppler-derived IRVF patterns and venous impedance index with RAP and their utility in predicting diuretic response and adverse outcomes. Furthermore, we assessed the tricuspid annular plane systolic excursion/systolic PAP ratio as a parameter of right ventricle–pulmonary artery coupling, which was recently demonstrated to be associated with prognosis in patients with pulmonary arterial hypertension and HF with preserved ejection fraction.^{31,32} The association of the tricuspid annular plane systolic excursion/systolic PAP ratio and RVSI further emphasizes the meaning of RVSI as a marker of renal congestion, as it mirrors not only RV failure but also right ventricle–pulmonary artery uncoupling when afterload exceeds contractility.

IRVF depends on extrinsic factors (interstitial pressure and intra-abdominal pressure) and intravenous pressure, which is highly dependent on RAP.^{33–35} Under physiological conditions, intrarenal veins exhibit continuous flow independent of renal function,^{36,37} with superimposed biphasic forward velocities that peak during systole (reflecting right atrial filling during RV ejection) and diastole (reflecting RAP release after the tricuspid valve opens and RV filling occurs). With increasing RAP, intrarenal veins become less compliant, dampening the continuous flow to a discontinuous ($RVSI>0$) flow and increasing prominence of the superimposed biphasic forward velocities. Further increases in RAP may ultimately lead to a diastolic-only (monophasic) flow pattern, in which renal venous outflow may exclusively depend on RV filling. Of note, the increase in RAP during end-diastole (corresponding to atrial contraction) can be transmitted to the renal veins, potentially causing a reversal of vein flow, as recently described³⁸; this may have been masked by the arterial waveforms in our analysis of interlobar arteries and veins.

Deterioration of renal function in right HF appears to be mainly hemodynamic (congestive), independent of PH subtype, and associated with activation of the neurohormonal system and fluid overload. This type of congestive nephropathy can be described as a gradual decrease of renal function as RVSI worsens, with no proteinuria even at severe congestion. Interestingly, we see no significant changes in creatinine, eGFR, or cystatin C in patients with RVSI in the first tertile compared with normal RVSI ($=0$). This could be explained by renal lymphatic flow increasing dramatically with early congestion, consequently preventing an increase in renal interstitial pressure until full saturation,^{39,40} and suggests that

Table 2. Predictors of Clinical End Points Identified by the Cox Proportional Hazards Model

Predictor	Univariate		Multiple	
	HR (95% CI)	P Value	HR (95% CI)	P Value
PH-related morbidity and death from any cause				
RVSI tertiles	20.57 (9.03–46.87)	<0.0001		0.0015
First tertile group vs RVSI 0	2.31 (1.06–5.05)	0.0363	2.30 (0.95–5.53)	0.064
Second tertile group vs RVSI 0	3.63 (1.71–7.65)	0.0007	3.41 (1.49–7.81)	0.0037
Third tertile group vs RVSI 0	8.70 (4.33–17.48)	<0.0001	4.72 (2.10–10.59)	<0.0001
Congestion stages	2.00 (1.63–2.44)	<0.0001		0.0012
Stage 1 vs stage 0	2.65 (1.29–5.44)	0.0078	2.61 (1.18–5.80)	0.0182
Stage 2 vs stage 0	6.35 (3.08–13.09)	<0.0001	4.90 (2.15–11.18)	<0.0001
Stage 3 vs stage 0	8.45 (3.98–17.96)	<0.0001	4.07 (1.68–9.85)	0.0019
Uric acid	1.25 (1.16–1.34)	<0.0001	1.15 (1.05–1.26)	0.0017
Atrial fibrillation	2.56 (1.68–3.88)	<0.0001	1.94 (1.05–3.56)	0.0355
6MWD	0.997 (0.996–0.999)	0.0006	0.997 (0.995–0.999)	0.0099
LA diameter	1.07 (1.04–1.10)	<0.0001	1.05 (1.01–1.10)	0.0301
Age	1.02 (1.00–1.03)	0.0439	0.98 (0.96–1.00)	0.079
Unscheduled hospitalization due to fluid overload				
RVSI tertiles	1.71 (1.48–1.98)	<0.0001		0.0016
First tertile group vs RVSI 0	6.49 (1.42–29.64)	0.0157	5.50 (1.09–27.85)	0.0395
Second tertile group vs RVSI 0	10.98 (2.52–47.76)	0.0014	6.27 (1.36–28.96)	0.0187
Third tertile group vs RVSI 0	35.60 (8.54–148.38)	<0.0001	13.01 (2.95–57.34)	0.0007
Congestion stages	2.49 (1.94–3.20)	<0.0001		0.0193
Stage 1 vs stage 0	7.36 (1.71–31.72)	0.0074	5.01 (1.14–22.07)	0.0334
Stage 2 vs stage 0	25.51 (6.05–107.67)	<0.0001	8.84 (1.98–39.46)	0.0043
Stage 3 vs stage 0	32.17 (7.44–139.09)	<0.0001	5.06 (1.02–25.20)	0.0478
Uric acid	1.29 (1.19–1.41)	<0.0001	1.27 (1.13–1.43)	<0.0001
PCWP	1.08 (1.05–1.11)	<0.0001	1.04 (1.01–1.08)	0.0159
Urine α 1MCR	1.01 (1.01–1.02)	<0.0001	1.01 (1.00–1.02)	0.0262
Atrial fibrillation	4.05 (2.47–6.63)	<0.0001	1.88 (1.00–3.54)	0.0510
6MWD	0.996 (0.994–0.998)	<0.0001	0.99 (0.99–1.00)	0.0006
RA area	1.11 (1.07–1.14)	<0.0001	1.05 (1.00–1.10)	0.0477
Urine feNa	1.21 (1.07–1.36)	0.0017	0.82 (0.67–1.00)	0.0547
NYHA classification	1.81 (1.24–2.64)	0.0022	0.60 (0.34–1.05)	0.074
Escalation of PH-specific therapy				
Mixed venous oxygen saturation	0.92 (0.90–0.95)	<0.0001	0.96 (0.93–1.00)	0.0403
Uric acid	1.26 (1.16–1.36)	<0.0001	1.31 (1.02–1.26)	0.0242
RVSI tertiles	1.43 (1.26–1.63)	<0.0001		0.0186
First tertile group vs RVSI 0	2.16 (0.89–5.24)	0.087	1.89 (0.68–5.27)	0.2241
Second tertile group vs RVSI 0	3.52 (1.53–8.07)	0.0030	2.91 (1.13–7.51)	0.0271
Third tertile group vs RVSI 0	7.03 (3.22–15.35)	<0.0001	4.29 (1.63–11.27)	0.0031
Congestion stages	1.86 (1.49–2.33)	<0.0001		0.0106
Stage 1 vs stage 0	2.37 (1.05–5.35)	0.0373	2.13 (0.84–5.37)	0.110

Continued

Table 2. Continued

Predictor	Univariate		Multiple	
	HR (95% CI)	P Value	HR (95% CI)	P Value
Stage 2 vs stage 0	6.22 (2.79–13.87)	<0.0001	4.44 (1.74–11.32)	0.0018
Stage 3 vs stage 0	6.39 (2.73–14.97)	<0.0001	3.31 (1.13–9.70)	0.0293
E/e' ratio	1.07 (1.03–1.12)	0.0006	1.06 (1.01–1.10)	0.0138
6MWD	0.997 (0.995–0.999)	0.0013	0.998 (0.996–1.00)	0.073
LVEDD	0.95 (0.91–0.99)	0.0221	0.94 (0.89–0.99)	0.0179
All-cause mortality				
Mixed venous oxygen saturation	0.92 (0.88–0.96)	<0.0001	0.94 (0.89–0.99)	0.0120
RA area	1.10 (1.04–1.17)	0.0018	1.07 (1.01–1.15)	0.0341
NYHA classification	2.65 (1.30–5.41)	0.0074	1.97 (0.99–3.90)	0.0536

Table includes only variables that remained significant after Cox regression analysis. All available variables were included in the univariate analyses, and variables that were significant in the univariate analyses are provided in Tables S9–S12. α 1MCR indicates α 1-microglobulin-to-creatinine ratio; E/e' ratio, ratio of mitral inflow velocity to lateral annular relaxation velocity; feNa, fractional excretion of sodium; HR, hazard ratio; LA, left atrial; LVEDD, left ventricular end-diastolic diameter; NYHA, New York Heart Association; PCWP, pulmonary capillary wedge pressure; PH, pulmonary hypertension; RA, right atrial; RVSI, renal venous stasis index; 6MWD indicates 6-min walk distance.

an increase of RVSI from 0 to the first tertile may be a more sensitive marker to identify patients at risk for subsequent renal function decline than established biomarkers such as creatinine and cystatin C. Transmission of venous congestion to the renal veins is thought to impair GFR by increasing pressure in the efferent end of the glomerular capillary, which reduces glomerular–capillary hydrostatic pressure⁸; this can be reversed by lowering renal venous pressure in experimental models.³⁴ As an additional component, concomitant elevation of renal interstitial pressure is likely to reduce glomerular net ultrafiltration pressure by opposing glomerular–capillary hydrostatic pressure and to reduce renal blood flow, as shown by the significant increases in RRI in our population. Future studies need to determine whether therapies that reduce RAP will improve renal function and particularly which RAP range must be achieved to provide an acceptable balance of RV and renal function.

Our study has all the limitations of retrospective analyses of prospectively collected data. Limitations include its single-center design, selection bias, and moderate sample size and duration of follow-up. We assumed that the monophasic IRVF pattern reflects venous pressure release resulting from RV filling, but we did not determine end-diastolic filling pressures or RV volumes. In addition, entering RVSI and congestion stages to 1 Cox regression model was done for comparison of their prognostic value but may lead to overfitting of the model. All echocardiography data were collected 1 day before RHC. Although PH-specific therapy was not initiated or changed in the interval between these assessments, some patients received additional diuretics when fluid overload was present, which limits the interpretation of echocardiography relative to RHC data. Renal venous congestion does not necessarily indicate right HF because tricuspid insufficiency with intact RV

function may also induce congestion, and discontinuous IRVF patterns have been described in obstructive nephropathy,⁴¹ where they are at least partly explained by increased renal interstitial pressure subsequent to ureter obstruction.

Our study confirmed the prognostic relevance of renal venous congestion, and the novel RVSI in particular showed promise as a simple, noninvasive, and objective Doppler measure. RVSI and IRVF patterns may be useful to identify patients who are likely to experience adverse outcomes. Longitudinal studies are needed to clarify their roles in the management of HF.

Conclusions

Our analyses of patients undergoing RHC present RVSI as a novel Doppler measurement of renal congestion that may be superior to IRVF patterns in predicting outcome in patients with PH. Further studies are needed to validate our findings and assess the utility of RVSI in PH management.

Acknowledgments

The authors thank the nursing staff of the pulmonology and nephrology departments for their hard work and commitment to patient well-being. Without their support, this work would not have been possible. Special thanks are extended to Susanne Wissgott and Isabell Heineke for their efforts in patient recruitment. Editorial assistance was provided by Claire Mulligan, PhD (Beacon Medical Communications Ltd, Brighton, UK), funded by the University of Giessen. The authors shared study design, data collection, data analysis, and data interpretation, as well as preparation, review, and approval of the article. The corresponding author had full access to all the data in the study and had final responsibility for the decision to submit for study concept and design: Husain-Syed, Birk, Ronco, Schörmann, Gall, and Ghofrani. Gall and Ghofrani conceived the

study concept and share the senior authorship of the article. Literature research and clinical advice: Birk, Ronco, Bauer, Walmrath, Seeger and McCullough. Acquisition, analysis, or interpretation of data: Husain-Syed, Birk, Ronco, Schörmann, Tello, Richter, Wilhelm, Sommer, Steyerberg, Bauer, McCullough, Gall, Ghofrani. Drafting of the article: Husain-Syed, Birk, Ronco, Wilhelm, Seeger, McCullough, Gall, and Ghofrani. Critical revision of the article for important intellectual content: Husain-Syed, Birk, Ronco, Schörmann, Tello, Richter, Wilhelm, Sommer, Steyerberg, Bauer, Walmrath, Seeger, McCullough, Gall, and Ghofrani. Adjudication of renal function: Husain-Syed, Birk, Ronco. Adjudication of IRVF patterns: Husain-Syed, Bauer, Ghofrani. Adjudication of end point: Walmrath, Ronco, Seeger. Statistical analysis: Wilhelm, Steyerberg, Gall. Study supervision: Gall and Ghofrani.

Sources of Funding

This study was funded by the German Research Foundation Collaborative Research Centers 1213, projects B08 and B07. The funder of the study had no role in the study design; the collection, analysis, and interpretation of data; writing of the report; and the decision to submit the article for publication.

Disclosures

Seeger disclosed personal fees for consulting from Bayer Pharma AG, from Liquidia Technologies, Inc, and from United Therapeutics Corporation outside the submitted work. Gall discloses personal fees and nonfinancial support from Actelion, AstraZeneca, Bayer, BMS, GlaxoSmithKline, Janssen Cilag, Lilly, MSD, Novartis, Pfizer, and United Therapeutics/OMT outside the submitted work. Ghofrani discloses grants from the German Research Foundation during the conduct of the study and personal fees from Actelion, Bayer, GSK, Novartis, Pfizer, Bellerophon Pulse Technologies, and MSD Merck Sharpe & Dohme outside the submitted work. The remaining authors have no disclosures to report.

References

1. Ponikowski P, Anker SD, AlHabib KF, Cowie MR, Force TL, Hu S, Jaarsma T, Krum H, Rastogi V, Rohde LE, Samal UC, Shimokawa H, Budi Siswanto B, Sliwa K, Filippatos G. Heart failure: preventing disease and death worldwide. *ESC Heart Fail*. 2014;1:4–25.
2. Ambrosy AP, Fonarow GC, Butler J, Chioncel O, Greene SJ, Vaduganathan M, Nodari S, Lam CSP, Sato N, Shah AN, Gheorghiade M. The global health and economic burden of hospitalizations for heart failure: lessons learned from hospitalized heart failure registries. *J Am Coll Cardiol*. 2014;63:1123–1133.
3. Mullens W, Abrahams Z, Francis GS, Sokos G, Taylor DO, Starling RC, Young JB, Tang WH. Importance of venous congestion for worsening of renal function in advanced decompensated heart failure. *J Am Coll Cardiol*. 2009;53:589–96.
4. Damman K, van Deursen VM, Navis G, Voors AA, van Veldhuisen DJ, Hillege HL. Increased central venous pressure is associated with impaired renal function and mortality in a broad spectrum of patients with cardiovascular disease. *J Am Coll Cardiol*. 2009;53:582–8.
5. Abraham WT, Adamson PB, Bourge RC, Aaron MF, Costanzo MR, Stevenson LW, Strickland W, Neelagaru S, Raval N, Krueger S, Weiner S, Shavelle D, Jeffries B, Yavad JS; CHAMPION Trial Study Group. Wireless pulmonary artery haemodynamic monitoring in chronic heart failure: a randomised controlled trial. *Lancet*. 2011;377:658–66.
6. Mullens W, Abrahams Z, Skouri HN, Francis GS, Taylor DO, Starling RC, Paganini E, Tang WH. Elevated intra-abdominal pressure in acute decompensated heart failure: a potential contributor to worsening renal function? *J Am Coll Cardiol*. 2008;51:300–6.
7. Husain-Syed F, McCullough PA, Birk HW, Renker M, Brocca A, Seeger W, Ronco C. Cardio-Pulmonary-Renal Interactions: a Multidisciplinary Approach. *J Am Coll Cardiol*. 2015;65:2433–48.
8. Jessup M, Costanzo MR. The cardiorenal syndrome: do we need a change of strategy or a change of tactics? *J Am Coll Cardiol*. 2009;53:597–9.
9. Iida N, Seo Y, Sai S, Machino-Ohtsuka T, Yamamoto M, Ishizu T, Kawakami Y, Aonuma K. Clinical Implications of Intrarenal Hemodynamic Evaluation by Doppler Ultrasonography in Heart Failure. *JACC Heart failure*. 2016;4:674–82.
10. Nijst P, Martens P, Dupont M, Tang WHW, Mullens W. Intrarenal Flow Alterations During Transition From Euvolemia to Intravascular Volume Expansion in Heart Failure Patients. *JACC Heart failure*. 2017;5:672–681.
11. Puzzovivo A, Monitillo F, Guida P, Leone M, Rizzo C, Grande D, Ciccone MM, Iacoviello M. Renal venous pattern: a new parameter for predicting prognosis in heart failure outpatients. *J Cardiovasc Dev Dis*. 2018;5:E52.
12. Beaubien-Souligny W, Benkreira A, Robillard P, Bouabdallaoui N, Chasse M, Desjardins G, Lamarche Y, White M, Bouchard J, Denault A. Alterations in Portal Vein Flow and Intrarenal Venous Flow Are Associated With Acute Kidney Injury After Cardiac Surgery: A Prospective Observational Cohort Study. *J Am Heart Assoc*. 2018;7:e009961. doi:10.1161/JAHA.118.009961.
13. Mehra MR, Park MH, Landzberg MJ, Lala A, Waxman AB; International Right Heart Failure Foundation Scientific Working Group. Right heart failure: toward a common language. *J Heart Lung Transplant*. 2014;33:123–6.
14. Galie N, Humbert M, Vachiery JL, Gibbs S, Lang I, Torbicki A, Simonneau G, Peacock A, Vonk Noordegraaf A, Beghetti M, Ghofrani A, Gomez Sanchez MA, Hansmann G, Klepetko W, Lancellotti P, Matucci M, McDonagh T, Pierard LA, Trindade PT, Zompatori M, Hoeper M, Aboyans V, Vaz Carneiro A, Achenbach S, Agewall S, Allanore Y, Asteggiano R, Paolo Badano L, Albert Barbera J, Bouvaist H, Bueno H, Byrne RA, Carerj S, Castro G, Erol C, Falk V, Funck-Brentano C, Gorenflo M, Granton J, Jung B, Kiely DG, Kirchhof P, Kjellstrom B, Landmesser U, Lekakis J, Lionis C, Lip GY, Orfanos SE, Park MH, Piepoli MF, Ponikowski P, Revel MP, Rigau D, Rosenkranz S, Voller H, Luis Zamora J. 2015 ESC/ERS guidelines for the diagnosis and treatment of pulmonary hypertension: the joint task force for the diagnosis and treatment of pulmonary hypertension of the European Society of Cardiology (ESC) and the European Respiratory Society (ERS); endorsed by: association for European Paediatric and Congenital Cardiology (AEPC), International Society for Heart and Lung Transplantation (ISHLT). *Eur Heart J*. 2016;37:67–119.
15. Ponikowski P, Voors AA, Anker SD, Bueno H, Cleland JG, Coats AJ, Falk V, Gonzalez-Juanatey JR, Harjola VP, Jankowska EA, Jessup M, Linde C, Nihoyannopoulos P, Parissis JT, Pieske B, Riley JP, Rosano GM, Ruilope LM, Ruschitzka F, Rutten FH, van der Meer P; ESC Scientific Document Group. 2016 ESC Guidelines for the diagnosis and treatment of acute and chronic heart failure: the Task Force for the diagnosis and treatment of acute and chronic heart failure of the European Society of Cardiology (ESC). Developed with the special contribution of the Heart Failure Association (HFA) of the ESC. *Eur Heart J*. 2016;37:2129–200.
16. Kidney Disease: Improving Global Outcomes (KDIGO) Chronic Kidney Disease Work Group. KDIGO. Clinical Practice Guideline for the Evaluation and Management of Chronic Kidney Disease. *Kidney Int Suppl*. 2012;2013:1–150.
17. Kidney Disease: Improving Global Outcomes (KDIGO) Acute Kidney Injury Work Group. KDIGO clinical practice guideline for acute kidney injury. *Kidney Int Suppl*. 2012;2:1–138.
18. Gall H, Felix JF, Schneck FK, Milger K, Sommer N, Voswinckel R, Franco OH, Hofman A, Schermuly RT, Weissmann N, Grimminger F, Seeger W, Ghofrani HA. The Giessen Pulmonary Hypertension Registry: survival in pulmonary hypertension subgroups. *J Heart Lung Transplant*. 2017;36:957–967.
19. Li JC, Jiang YX, Zhang SY, Wang L, Ouyang YS, Qi ZH. Evaluation of renal artery stenosis with hemodynamic parameters of Doppler sonography. *J Vasc Surg*. 2008;48:323–8.
20. Sugiura T, Wada A. Resistive index predicts renal prognosis in chronic kidney disease. *Nephrol Dial Transplant*. 2009;24:2780–5.
21. Rudski LG, Lai WW, Afilalo J, Hua L, Handschumacher MD, Chandrasekaran K, Solomon SD, Louie EK, Schiller NB. Guidelines for the echocardiographic assessment of the right heart in adults: a report from the American Society of Echocardiography endorsed by the European Association of Echocardiography, a registered branch of the European Society of Cardiology, and the Canadian Society of Echocardiography. *J Am Soc Echocardiogr*. 2010;23:685–713;quiz 786–788.
22. Mohmand H, Goldfarb S. Renal dysfunction associated with intra-abdominal hypertension and the abdominal compartment syndrome. *J Am Soc Nephrol*. 2011;22:615–21.
23. ATS Committee on Proficiency Standards for Clinical Pulmonary Function Laboratories. ATS statement: guidelines for the six-minute walk test. *Am J Respir Crit Care Med*. 2002;166:111–117.

24. Vargo DL, Kramer WG, Black PK, Smith WB, Serpas T, Brater DC. Bioavailability, pharmacokinetics, and pharmacodynamics of torsemide and furosemide in patients with congestive heart failure. *Clin Pharmacol Therap*. 1995;57:601–9.
25. Levey AS, Stevens LA, Schmid CH, Zhang YL, Castro AF III, Feldman HI, Kusek JW, Eggers P, Van Lente F, Greene T, Coresh J; CKD-EPI (Chronic Kidney Disease Epidemiology Collaboration). A new equation to estimate glomerular filtration rate. *Ann Intern Med*. 2009;150:604–12.
26. Inker LA, Schmid CH, Tighiouart H, Eckfeldt JH, Feldman HI, Greene T, Kusek JW, Manzi J, Van Lente F, Zhang YL, Coresh J, Levey AS; CKD-EPI Investigators. Estimating glomerular filtration rate from serum creatinine and cystatin C. *New Engl J Med*. 2012;367:20–9.
27. R Core Team. *R: A Language and Environment for Statistical Computing*. Vienna, Austria: R Foundation for Statistical Computing; Version 3.5.1. 2018. Available at: <https://www.R-project.org/>. Accessed November 20, 2018.
28. Robin X, Turck N, Hainard A, Tiberti N, Lisacek F, Sanchez JC, Muller M. pROC: an open-source package for R and S+ to analyze and compare ROC curves. *BMC Bioinformatics*. 2011;12:77.
29. Qiu JC W, Lazarus R, Rosner B, Ma J. powerSurvEpi: power and sample size calculation for survival analysis of epidemiological studies. R package Version 0.1.0. 2018. Available at: <https://CRAN.R-project.org/package=powerSurvEpi>. Accessed November 20, 2018.
30. Freedman LS. Tables of the numbers of patients required in clinical trials using the log-rank test. *Stat Med*. 1982;1:121–129.
31. Tello K, Axmann J, Ghofrani HA, Naeije R, Narcin N, Rieth A, Seeger W, Gall H, Richter MJ. Relevance of the TAPSE/PASP ratio in pulmonary arterial hypertension. *Int J Cardiol*. 2018;266:229–235.
32. Guazzi M, Dixon D, Labate V, Beussink-Nelson L, Bandera F, Cuttica MJ, Shah SJ. RV Contractile Function and its Coupling to Pulmonary Circulation in Heart Failure With Preserved Ejection Fraction: stratification of Clinical Phenotypes and Outcomes. *JACC Cardiovasc Imaging*. 2017;10:1211–1221.
33. Burnett JC Jr, Knox FG. Renal interstitial pressure and sodium excretion during renal vein constriction. *Am J Physiol*. 1980;238:F279–82.
34. Winton FR. The influence of venous pressure on the isolated mammalian kidney. *J Physiol*. 1931;72:49–61.
35. Winton FR. Arterial, Venous, Intrarenal, and Extrarenal Pressure Effects on Renal Blood Flow. *Circ Res*. 1964;15(SUPPL):103–9.
36. Avasthi PS, Greene ER, Scholler C, Fowler CR. Noninvasive diagnosis of renal vein thrombosis by ultrasonic echo-Doppler flowmetry. *Kidney Int*. 1983;23:882–7.
37. Jeong SH, Jung DC, Kim SH, Kim SH. Renal venous doppler ultrasonography in normal subjects and patients with diabetic nephropathy: value of venous impedance index measurements. *J Clin Ultrasound*. 2011;39:512–8.
38. Meier M, Johannes Jabs W, Guthmann M, Geppert G, Aydin A, Nitschke M. Sonographic Venous Velocity Index Identifies Patients with Chronic Kidney Disease and Severe Diastolic Dysfunction. *Ultrasound Int Open*. 2018;4:E142–E148.
39. Haddy FJ, Scott J, Fleishman M, Emanuel D. Effect of change in renal venous pressure upon renal vascular resistance, urine and lymph flow rates. *Am J Physiol*. 1958;195:97–110.
40. Lebric SJ, Mayerson HS. Influence of elevated venous pressure on flow and composition of renal lymph. *Am J Physiol*. 1960;198:1037–40.
41. Bateman GA, Cuganesan R. Renal vein Doppler sonography of obstructive uropathy. *AJR Am J Roentgenol*. 2002;178:921–5.

SUPPLEMENTAL MATERIAL

Data S1.

SUPPLEMENTAL METHODS

Study design and participants

Data collection

Clinical variables were abstracted from patient medical records. All clinical and laboratory data, including patient demographics, were collected and stored in a password-protected dataset.

Right heart catheterization (RHC)

All RHC measures were derived at end-expiration, and reported values represent the average of 5 to 10 cardiac cycles. Cardiac output (average of three cycles with <10% variation in patients in sinus rhythm and five cardiac cycles in patients with atrial fibrillation) was derived by both thermodilution and the Fick method using nomograms for oxygen uptake in conjunction with the Fick method. If patients did not have supplemental oxygen therapy, the direct Fick method was performed directly after oxygen uptake assessment. When a discrepancy was present between both methods, cardiac output was reported by direct Fick; if direct Fick measurement was not possible, thermodilution was used. Pulmonary vascular resistance and cardiac index were calculated as described previously (pulmonary vascular resistance=[mean pulmonary arterial pressure–pulmonary capillary wedge pressure]/cardiac output; cardiac index=[cardiac output/body surface area]).¹

Bioimpedance spectroscopy

Bioimpedance is based on the principle that the body acts as a circuit with a given resistance (opposition of current flow through intracellular and extracellular solutions [Ri and Re]) and reactance (the capacitance of cells to store energy [Xc]).² The volume of the body fluid component is largely reflected in the resistance, whereas reactance might represent cell membrane integrity. The impedance is composed of the sum of resistance and reactance ($\sqrt{R^2 + Xc^2}$).³ Another parameter that can be derived is the phase angle, which is the arc tangent of Xc/R. When a current passes through cells, a portion of the electrical current is stored and subsequently released in a different phase, termed “phase angle”. The phase angle is related to the ability of cells to function as capacitors, which is dependent on the integrity of the cell membrane and cellular health. Bioimpedance data from the study population are provided in Table S4.

The three-compartment model of the BCM Body Composition Monitor has been validated against standard reference methods for assessment of fluid status and body composition in patients undergoing hemodialysis and peritoneal dialysis, albeit partly against gold standard techniques in healthy controls only.^{4–7} BCM has been shown to be valid in different ethnicities⁵, and measures impedance at 50 different frequencies between 5 kHz and 1 MHz. Reproducibility of BCM-derived parameters is high, with a coefficient of variation for the inter-observer variability for extracellular water and total body water around 1.2% in studies⁸ performed in patients undergoing hemodialysis. Therefore, only one BCM measurement was performed in each individual patient. BCM results are normalized by sex and patient height. According to the manufacturer’s recommendations we excluded patients if they had an unipolar pacemaker, while there were no limitations for patients with stents or bipolar pacemakers.⁹ For measurement, the skin was cleansed with alcohol, then the electrodes were attached to one hand and one foot at the ipsilateral side, after the patient had been supine for at least 5 minutes and not touching any metal objects.

Hydration status (expressed in Liters) was derived from the impedance data based on a physiologic tissue model that separates the body into three compartments⁴: surplus water, normohydrated lean tissue, and fat tissue. Hydration status represents the difference between the measured amount of extracellular water and the amount of water expected in normohydrated tissue conditions. Patients are considered ‘dehydrated’ or ‘overhydrated’ when their absolute hydration status is below the 10th or above the 90th percentile of the normal, presumed healthy, reference population, respectively (corresponding to 1.1 L of negative or positive hydration status, respectively).^{10, 11} Due to bio-physical reasons, bioimpedance spectroscopy does not measure sequestered fluid in the trunk, and presence of pleural effusion and ascites was documented by ultrasound.¹² Lean tissue mass represents the body mass without adipose tissue and excess extracellular water (fluid overload). Fat represents the mass of adipose lipids in the body. Lean tissue mass and fat are provided in kilograms as well as in relation to body weight (%). Lean tissue index is calculated as the quotient of lean tissue mass/height. Fat tissue index is defined as the quotient of adipose tissue mass/height. Adipose tissue mass is the mass of the adipose tissue, including the adipose water. Body cell mass represents the cellular, metabolically active body mass, excluding the extracellular fluid in the metabolically active tissue.¹²

Intra-abdominal pressure measurement

Intra-abdominal pressure was measured with a standard Foley catheter, which was connected to a pressure transducer placed in-line with the iliac crest at the midaxillary line. The Foley catheter was flushed with a maximal instillation volume of 50 mL sterile saline via the aspiration port of the Foley catheter with the drainage

tube clamped to allow a fluid-filled column to develop up into the bladder. A pressure transducer was then inserted in the aspiration port, and the pressure was measured. The intra-abdominal pressure was expressed in mm Hg and was measured at end-expiration in the supine position, ensuring that abdominal muscle contractions were absent.

Laboratory methods

Blood and urine samples were centrifuged for 10 minutes at 3000xg and 5 minutes at 500xg, respectively. Samples were processed within 30 minutes of collection.

B-type natriuretic peptide (BNP) and parathormone were measured by the chemiluminescence method on an Advia Centaur XPT analyzer (Siemens Healthcare GmbH, Erlangen, Germany). BNP >35 pg/mL was taken as the cut-off for diagnosing chronic heart failure.¹³ Copeptin was measured by the Time-Resolve-Amplified Cryptate Emission method on a Brahms Kryptor Compact Plus (Thermo Fisher Scientific, MA, USA). The range of copeptin, a surrogate marker for proarginine vasopressin release and neurohormonal activation, in healthy individuals has been recently described as 4.2 [9.5] pmol/L.¹⁴ Serum aldosterone was measured by the radioimmunological method on a Multi Crystal LB 2111 Gamma Counter (Berthold Technologies, Bad Wildbach, Germany). Urine sodium-to-potassium ratio <2 was considered as a marker of hyperaldosteronism. Urine fractional excretion of sodium <1% was considered as a marker of sodium retention. Cystatin C was measured by the immunoturbidimetric method on an AU5800 Chemistry Analyzer (Beckman Coulter, California, USA) with reference material ERM-DA471/IFCC (distributed by the European Joint Research Institute for Reference Materials and Measurements, Geil, Belgium).¹⁵ Creatinine was measured by the photometric-enzymatic method on an Advia Centaur XPT analyzer, with calibration to isotope dilution mass spectrometry reference measurements. Blood urea nitrogen-to-creatinine ratio >20 was considered as a marker of neurohormonally mediated disproportionate reabsorption of urea compared with that of creatinine.¹⁶ Creatinine clearance was calculated as: urine creatinine (mg/dL) x urine volume (mL) x 1.73 (m²)/1440 min x serum creatinine (mg/dL) x body surface area (m²). For calculation of urea clearance, creatinine was substituted with urea.

Proteinuria was measured using a colorimetric method with pyrogallol red on an AU5800 Chemistry Analyzer. Albuminuria was measured by the immunoturbidimetric method on a Advia Centaur XPT, and alpha 1-microglobulin was measured by the immunonephelometric method on a BNII analyzer (Siemens Healthcare GmbH, Erlangen, Germany). Protein-to creatinine ratio, albumin-to-creatinine ratio, and alpha 1-microglobulin-to-creatinine ratio (all reported in units of mg/g creatinine) were then calculated. Microalbuminuria and increased tubular proteinuria (alpha 1 microglobulin) were defined as values ≥ 30 mg/g and ≥ 20 mg/g creatinine, respectively.^{17, 18} Positive acanthocyturia, a diagnostic criterion of glomerulonephritis, was defined as $\geq 5\%$ acanthocytes in centrifuged urinary sediment detected with a phase-contrast microscope Eclipse Ci-L (Nikon, Tokyo, Japan).¹⁹ Sterile leukocyturia, associated with interstitial nephritis, nephrolithiasis, uroepithelial tumors, and infection with atypical organisms, was defined as a positive urinary dip stick test for leukocyte esterase in combination with a negative urine culture.²⁰

Renal replacement therapy (RRT)

Patients with fluid overload received a stepped pharmacological diuretic therapy including adjustable doses of intravenous loop diuretic agents, thiazide diuretic agents, and aldosterone antagonists. Patients who fulfilled the criteria for diuretic resistance despite the stepped pharmacological therapy were transferred to RRT, as were patients who developed stage 3 acute kidney injury with fluid overload or a life-threatening complication (eg, pulmonary edema).²¹ Modality of RRT was based on illness acuteness, patient preference, and co-morbidities (eg, presence of ascites). In general, peritoneal dialysis (conventional surgical technique; peritoneal dialysis catheter type Oreopoulous-Zellermann) was the preferred modality for patients with HF, except patients with life-threatening indications or cardiovascular instability, for whom slow extended daily hemodialysis with the GENIUS® dialysis system (Fresenius Medical Care, Bad Homburg, Germany) was preferred.

Table S1. ICC for RVSI measured by two independent nephrologists.

	Intraclass correlation*	95% confidence interval		F test with true value 0			
		Lower bound	Upper bound	Value	df1	df2	Significance
Inter-observer reliability							
Single measures	0.978†	0.973	0.982	178.709	204	612	0.000
Average measures	0.994‡	0.993	0.996	178.709	204	612	0.000
Intra-observer reliability							
TS – single measures	1.000†	1.000	1.000		204		
TS – average measures	1.000‡	1.000	1.000		204		
FH-S – single measures	1.000†	1.000	1.000	5302.258	204	204	0.000
FH-S – average measures	1.000‡	1.000	1.000	5302.258	204	204	0.000
Two-way mixed effects model where people effects are random and measures effects are fixed.							

Two-way mixed effects model where people effects are random and measures effects are fixed.

*Type A ICCs using an absolute agreement definition for inter-observer reliability; Type C ICCs using a consistency definition for intra-observer reliability.

†The estimator is the same, whether the interaction effect is present or not.

‡This estimate is computed assuming the interaction effect is absent, because it is not estimable otherwise.

df=degrees of freedom; ICC=intraclass correlation coefficient; RVSI=renal venous stasis index.

Table S2. Classification of the RHC Cohort According to PH Subcategories.

	n (%)
No PH	40 (100)
Disease control	27 (67.5)
HF with preserved ejection fraction	13 (32.5)
Group 1 (PAH)	46 (100)
Idiopathic PAH	27 (58.7)
Connective tissue disease	8 (17.4)
Congenital systemic-to-pulmonary shunts	6 (13.0)
Porto-pulmonary PH	5 (10.9)
Group 2 (PH due to left heart disease)	30 (100)
PH-HF with preserved ejection fraction	30 (100)
Group 3 (PH due to lung disease and/or hypoxemia)	41 (100)
Chronic obstructive pulmonary disease	22 (53.7)
Interstitial lung disease	15 (36.6)
Sleep-disordered breathing	4 (9.8)
Group 4 (chronic thromboembolic PH)	34 (100)
Group 5 (PH with unclear multifactorial mechanisms)	14 (100)
Sarcoidosis	9 (64.3)
Churg-Strauss syndrome	1 (1.6)
Unknown mechanisms	4 (28.6)

HF denotes heart failure, PAH pulmonary arterial hypertension, PH pulmonary hypertension, and RHC right heart catheterization

Table S3. Clinical characteristics, invasive hemodynamics, echocardiographic data, renal function, and neurohormonal and hydration status stratified according to congestion stages as determined by intrarenal venous flow patterns.

	All patients (n=205)	No congestion (n=59)	Stage 1 congestion (n=77)	Stage 2 congestion (n=44)	Stage 3 congestion (n=25)	p value*
Baseline clinical data						
6MWD, m	277.23±136.05	309.76±118.16	296.83±142.97	224.55±127.15	232.80±137.57	0.0022
NYHA classification, n (%)						0.078
1–2	44 (21.5)	15 (25.4)	22 (28.6)	4 (9.1)	3 (12)	
3–4	161 (78.5)	44 (74.6)	45 (71.4)	40 (90.9)	22 (88)	
Oxygen supply, n (%)	118 (57.6)	28 (47.5)	45 (58.4)	33 (75.0)	12 (48.0)	0.0306
Maintenance therapy						
ACEi or ARB, n (%)	83 (40.5)	23 (39.0)	33 (42.9)	13 (29.5)	14 (56.0)	0.178
Loop diuretic dose, mg/day	40.0 [0.0–60.0]	20.0 [0.0–40.0]	20.0 [0.0–45.0]	40.0 [0.0–80.0]	80.0 [40.0–200.0]	<0.0001
Thiazide diuretic, n (%)	72 (35.1)	18 (30.5)	27 (35.1)	17 (38.6)	10 (40.0)	0.789
Aldosterone antagonist, n (%)	76 (37.1)	16 (27.1)	30 (39.0)	17 (38.6)	13 (52.0)	0.168
Triamterene, n (%)	5 (2.4)	0 (0)	3 (3.9)	2 (4.5)	0 (0)	0.307
PH-specific therapy, n (%)						0.433
Treatment-naïve	116 (56.6)	42 (71.2)	36 (46.8)	24 (54.5)	14 (56.0)	
Monotherapy	49 (23.9)	8 (13.6)	23 (29.9)	11 (25.0)	7 (28.0)	
Dual therapy	28 (13.7)	6 (10.2)	13 (16.9)	6 (13.6)	3 (12.0)	
Triple therapy	12 (5.9)	3 (5.1)	5 (6.5)	3 (6.8)	1 (4.0)	
Hemodynamics						
Mean PAP, mm Hg	34.84±14.63	24.10±9.62	37.14±15.02	42.84±12.33	39.00±13.11	<0.0001
PVR, dyn.s/cm ⁵	394 [214–604]	229 [110–420]	440 [277–600]	558 [293–829]	428 [245–750]	<0.0001
RAP, mm Hg	5.76±5.63	2.46±3.66	4.44±4.75	9.00±5.04	11.88±7.54	<0.0001
Cardiac index, L/min/m ²	2.73±0.98	2.98±1.01	2.76±1.00	2.47±0.70	2.48±1.13	0.0332
PCWP, mm Hg	9.0 [5.0–13.0]	7.0 [4.0–10.0]	9.0 [6.0–13.0]	10.5 [6.0–15.8]	12.0 [8.5–18.5]	<0.0001
Mixed venous oxygen saturation, %	63.76±8.35	66.70±6.42	65.11±6.59	59.83±9.70	59.60±10.63	<0.0001
Heart rate, beats/min	71.62±13.23	72.00±11.32	70.34±12.55	72.23±13.49	73.60±18.51	0.703
MAP, mm Hg†	84.25±11.57	85.22±10.28	83.71±12.18	85.69±13.06	81.09±9.48	0.375
Echocardiographic parameters						
<i>Right heart</i>						
TAPSE, mm	19.89±4.41	21.88±3.82	20.87±4.01	18.18±3.80	15.20±3.46	<0.0001
RV myocardial performance index (Tei index)	0.49±0.22	0.46±0.20	0.47±0.23	0.55±0.23	0.48±0.22	0.323
RV S', cm/s	11.60±3.52	12.95±3.31	12.18±3.20	10.17±3.23	9.08±3.43	<0.0001
TAPSE/Systolic PAP ratio	0.39±0.21	0.56±0.27	0.35±0.15	0.30±0.11	0.30±0.13	<0.0001
Tricuspid insufficiency, n (%)						0.0007
Mild	66 (32.2)	34 (57.6)	15 (19.5)	12 (27.3)	5 (20)	
Moderate	112 (54.6)	23 (39.0)	51 (66.2)	25 (56.8)	13 (52)	
Severe	25 (12.2)	1 (1.7)	10 (13.0)	7 (15.9)	7 (28)	
RA area, cm ²	18.89±6.72	14.14±6.30	18.87±5.70	20.99±6.24	24.16±6.60	<0.0001
RV diameter, mm	40.78±8.08	37.93±7.38	40.43±6.68	43.40±8.86	44.04±9.86	0.0009
IVC, cm	2.27±0.49	2.01±0.52	2.30±0.44	2.45±0.31	2.51±0.54	<0.0001
<i>Left heart</i>						
LVEF, %	60.0 [60.0–65.0]	60 [60.0–65.0]	60 [60.0–65.0]	60 [55.0–65.0]	60 [52.5–60.5]	0.0552

LA diameter, mm	41.98±6.86	39.78±6.35	40.65±6.51	43.17±6.12	48.56±5.85	<0.0001
LVEDD, mm	46.03±5.59	46.28±4.73	45.10±5.45	46.24±7.01	47.84±4.85	0.184
E/e' ratio	12.98±5.34	11.07±3.52	12.96±4.12	13.80±6.52	16.42±8.07	0.0007
Renal function						
Serum creatinine, mg/dL‡	1.01±0.45	0.92±0.40	0.86±0.26	1.13±0.53	1.44±0.52	<0.0001
Cystatin C, mg/L	1.10 [0.91–1.52]	0.98 [0.81–1.24]	1.06 [0.88–1.29]	1.33 [1.03–1.64]	1.83 [1.34–2.22]	<0.0001
Urea, mg/dL§	47.44±35.85	40.97±26.71	37.12±17.31	59.84±56.61	72.72±32.68	<0.0001
eGFR (CKD-EPI creatinine equation), mL/min/1.73 m ²	74.45±26.12	80.07±24.51	81.57±21.49	67.25±27.96	51.96±24.92	<0.0001
eGFR (CKD-EPI creatinine-cystatin C equation), mL/min/1.73 m ² #	68.58±26.86	77.68±27.65	74.42±21.81	59.42±25.85	45.24±23.37	<0.0001
Renal filtration gradient, mm Hg**	69.30±12.46	73.70±10.60	70.36±12.08	67.64±13.00	58.61±10.42	<0.0001
Urine PCR, mg/g creatinine	58.8 [40.2–114.2]	51.5 [36.4–72.6]	55.3 [38.4–93.3]	70.3 [46.9–160.5]	116.2 [52.7–222.7]	0.0022
Urine ACR, mg/g creatinine	11.4 [6.3–29.7]	9.3 [5.2–16.0]	10.3 [6.2–22.2]	13.8 [8.1–45.8]	33.4 [11.3–223.7]	<0.0001
Urine α1MCR, mg/g creatinine	10.9 [6.0–19.1]	8.7 [5.1–16.5]	10.4 [5.9–19.0]	11.7 [7.0–25.3]	16.3 [8.3–40.1]	0.0283
Acanthocyturia, n (%)	7 (3.4)	2 (3.4)	3 (3.9)	2 (4.5)	0 (0)	0.775
Sterile leukocyturia, n (%)	2 (1.0)	1 (1.7)	0 (0)	1 (2.3)	0 (0)	0.555
Renal Doppler ultrasonography						
RVSI	0.11 [0.00–0.32]	0 [0.0–0.0]	0.10 [0.07–0.14]	0.33 [0.20–0.41]	0.56 [0.48–0.74]	<0.0001
Venous impedance index	0.84±0.26	0.44±0.12	1.00±0	1.00±0	1.00±0	<0.0001
RRI	0.71±0.07	0.69±0.08	0.70±0.07	0.74±0.06	0.75±0.06	<0.0001
Neurohormonal status						
BNP, pg/mL	138.0 [50.0–321.0]	46.0 [26.0–113.0]	150.0 [50.5–254.5]	303.0 [147.0–633.8]	534.0 [228.5–776.5]	<0.0001
Copeptin, pmol/L	11.1 [5.8–23.3]	9.1 [4.6–16.0]	7.9 [5.2–15.4]	18.8 [7.3–29.8]	27.7 [13.7–50.7]	<0.0001
Sodium, mmol/L	139.56±3.07	139.32±3.15	139.57±2.80	140.59±2.86	138.24±3.60	0.0206
Urine FeNa, %	0.6 [0.4–1.3]	0.7 [0.4–1.2]	0.6 [0.4–1.1]	0.5 [0.4–1.5]	1.3 [0.5–2.5]	0.073
BUN-to-creatinine ratio	21.15±7.53	20.48±7.14	20.16±6.52	20.35±9.39	23.63±7.22	0.131
Aldosterone, ng/dL	5.60 [3.1–11.8]	4.90 [3.0–8.6]	4.90 [3.0–13.4]	6.15 [3.0–11.7]	10.50 [4.2–19.1]	0.0531
Potassium, mmol/L	3.67±0.42	3.65±0.40	3.65±0.41	3.77±0.453	3.66±0.42	0.591
Urine Na/K ratio	3.23±2.24	3.84±2.58	3.20±2.28	2.68±1.47	2.88±2.17	0.0532
Hydration status						
Ascites, n (%)	7 (3.4)	0 (0)	1 (1.3)	0 (0)	6 (24.0)	<0.0001
Pleural effusion, n (%)	17 (8.3)	3 (5.1)	5 (6.5)	2 (4.5)	7 (28.0)	0.0021
Peripheral edema, n (%)	60 (29.3)	12 (22.0)	22 (28.6)	15 (34.1)	10 (40.0)	0.335
Hydration status (as measured by bioimpedance), L	0.71±2.12	-0.14±1.41	0.78±2.24	1.16±2.09	1.70±2.55	0.0006
Total body water, L	37.78±7.47	37.93±8.71	36.78±6.99	39.46±7.20	37.73±5.86	0.359
ECW, L	17.55±3.30	17.36±3.79	16.94±3.01	18.50±3.38	18.31±2.32	0.069
ICW, L	20.28±4.53	20.56±5.24	19.85±4.43	20.97±4.24	19.83±3.32	0.574
ECW/ICW ratio	0.95±0.15	0.86±0.11	0.86±0.11	0.89±0.11	0.94±0.14	0.0204
Intra-abdominal pressure measurement						
Intra-abdominal pressure, mm Hg	7.0 [6.0–9.0]	6.0 [5.0–6.0]	7.0 [6.0–7.0]	9.0 [8.0–10.0]	11.0 [10.0–13.0]	<0.0001
Abdominal perfusion pressure, mm Hg††	76.78±11.81	79.46±10.38	77.04±12.09	76.67±12.96	69.85±9.67	0.0078

Values are mean±SD, median [interquartile range], or n (%).

*After application of the Bonferroni correction, $p < 0.0008$ was considered significant. †MAP was calculated as (systolic blood pressure+2x diastolic pressure)/3. ‡To convert the values for serum creatinine to $\mu\text{mol/L}$, multiply by 88.4. §eGFR was calculated with the CKD-EPI equation based on serum creatinine.²³ ||To convert the values for urea to BUN, multiply by 0.467. #eGFR was calculated with the CKD-EPI equation based on serum creatinine and cystatin C.²² **The renal filtration gradient was calculated as: $\text{MAP} - 2 \times \text{intra-abdominal pressure}$.²⁴ ††The abdominal perfusion pressure was calculated using the equation: $\text{MAP} - \text{intra-abdominal pressure}$.²⁴

6MWD=6-min walk distance; ACEi=angiotensin-converting enzyme inhibitor; ACR=albumin-to-creatinine ratio; $\alpha 1\text{MCR} = \alpha 1\text{-microglobulin-to-creatinine ratio}$; ARB=angiotensin receptor blocker; BUN=blood urea nitrogen; BNP=b-type natriuretic peptide; CKD-EPI=Chronic Kidney Disease Epidemiology Collaboration; ECW=extracellular water; E/e' ratio=ratio of mitral inflow velocity to lateral annular relaxation velocity; eGFR=estimated glomerular filtration rate; FeNa=fractional excretion of sodium; ICW=intracellular water; IVC=inferior vena cava; LA=left atrial; LVEDD=left ventricular end-diastolic diameter; LVEF=left ventricular ejection fraction; MAP=mean arterial pressure; Na/K=sodium/potassium; NYHA=New York Heart Association; PAP=pulmonary arterial pressure; PCR= protein-to-creatinine ratio; PCWP=pulmonary capillary wedge pressure; PH=pulmonary hypertension; PVR=pulmonary vascular resistance; RA=right atrial; RAP=right atrial pressure; RRI=renal resistive index; RV=right ventricular; RV S'=systolic annular tissue velocity of the lateral tricuspid annulus; RVSI=renal venous stasis index; TAPSE=tricuspid annular plane systolic excursion.

Table S4. Additional data on clinical characteristics, invasive hemodynamics, echocardiographic data, renal function, neurohormonal and hydration status according to congestion stages as determined by renal venous stasis index.

	All patients (n=205)	RVSI=0 (n=59)	RVSI tertiles			p value*
			First 0<RVSI≤0.12 (n=49)	Second >0.12<RVSI≤0.32 (n=48)	Third RVSI>0.32 (n=49)	
Maintenance therapy, n (%)						
Calcium channel blocker	46 (22.4)	10 (16.9)	11 (22.4)	14 (29.2)	11 (22.4)	0.518
Thiazide diuretic	72 (35.1)	18 (30.5)	18 (36.7)	17 (35.4)	19 (38.8)	0.826
Aldosterone antagonist	76 (37.1)	16 (27.1)	24 (49.0)	12 (25.0)	24 (49.0)	0.0095
Triamterene	5 (2.4)	0 (0)	2 (4.1)	3 (6.3)	0 (0)	0.103
Renal function, n (%)						
Acanthocyturia	7 (3.4)	2 (3.4)	2 (4.1)	1 (2.1)	2 (4.1)	0.942
Sterile leukocyturia	2 (1.0)	1 (1.7)	0 (0)	0 (0)	1 (2.0)	0.605
Neurohormonal status						
BUN-to-creatinine ratio	21.15±7.53	20.48±7.14	20.38±6.60	20.78±6.93	23.06±9.14	0.236
Aldosterone, ng/dL	5.60 [3.1–11.8]	4.9 [3.0–8.6]	5.9 [3.0–13.5]	4.7 [3.0–11.8]	7.2 [4.1–16.7]	0.0292
Urine Na/K ratio	3.23±2.24	3.84±2.58	3.34±2.35	2.87±1.76	2.76±1.98	0.0470
Hydration status, n (%)						
Total body water, L	37.78±7.47	37.93±8.71	36.50±7.30	37.82±6.19	38.92±7.11	0.495
Extracellular water, L	17.55±3.30	17.36±3.79	16.62±2.95	17.80±3.17	18.54±2.87	0.0450
Intracellular water, L	20.28±4.53	20.56±5.24	19.88±4.66	20.03±3.64	20.62±4.27	0.812

Values are mean±SD, median [interquartile range], or n (%).

*After application of the Bonferroni correction, p<0.004 was considered significant.

BUN=blood urea nitrogen; Na/K=sodium/potassium; PH=pulmonary hypertension; RVSI=renal venous stasis index.

Table S5. Correlation of RVSI with relevant parameters*.

	RVSI Correlation coefficient	p value†
Demographics		
Age	0.238	0.0006
Body mass index	– 0.025	0.720
Clinical variables		
6MWD	– 0.239	0.0006
Loop diuretic dose	0.369	<0.0001
Hemodynamics		
Mean PAP	0.472	<0.0001
PVR	0.321	<0.0001
RAP	0.584	<0.0001
Cardiac index	– 0.321	<0.0001
PCWP	0.404	<0.0001
Mixed venous oxygen saturation	– 0.391	<0.0001
Echocardiographic parameters		
<i>Right heart</i>		
TAPSE	– 0.456	<0.0001
RV myocardial performance index (Tei index)	0.037	0.672
RV S'	– 0.357	<0.0001
TAPSE/Systolic PAP ratio	– 0.332	<0.0001
RA area	0.471	<0.0001
RV diameter	0.272	<0.0001
IVC	0.355	<0.0001
<i>Left heart</i>		
LVEF	– 0.163	0.0201
LA diameter	0.404	<0.0001
E/e' ratio	0.250	0.0006
Renal function		
Serum creatinine	0.394	<0.0001
Urea	0.427	<0.0001
Cystatin C	0.462	<0.0001
eGFR (MDRD equation) ‡	– 0.365	<0.0001
eGFR (CKD-EPI creatinine equation)§	– 0.365	<0.0001
eGFR (CKD-EPI creatinine-cystatin C equation)	– 0.433	<0.0001
Renal filtration gradient#	– 0.327	<0.0001
Urine PCR	0.315	<0.0001
Urine ACR	0.341	<0.0001
Urine α 1MCR	0.233	0.0008
RRI	0.323	<0.0001
Neurohormonal status		
BNP	0.623	<0.0001
Copeptin	0.350	<0.0001
Hydration status		
Hydration status (as measured by bioimpedance)	0.301	<0.0001
ECW/ICW ratio	0.178	0.0141
Intra-abdominal pressure measurement		
Intra-abdominal pressure	0.772	<0.0001
Abdominal perfusion pressure**	– 0.214	0.0021

Pearson or Spearman correlation was considered as appropriate. *Relevant parameters were chosen based on their clinical role; in addition, parameters that showed a significant difference across RVSI tertiles (table 2) were included. †After application of the Bonferroni correction, $p < 0.0014$ was considered significant. ‡eGFR was calculated with the MDRD equation based on serum creatinine.²⁵ §eGFR was calculated with the CKD-EPI equation based on serum creatinine.²³ ||eGFR was calculated with the CKD-EPI equation based on serum creatinine and cystatin C.²² #The renal filtration gradient was calculated as: $\text{MAP} - 2 \times \text{intra-abdominal pressure}$.²⁴ **The abdominal perfusion pressure was calculated using the equation: $\text{MAP} - \text{intra-abdominal pressure}$.²⁴

6MWD=6-min walk distance; ACR=albumin-to-creatinine ratio; α 1MCR= α 1-microglobulin-to-creatinine ratio; CKD-EPI=Chronic Kidney Disease Epidemiology Collaboration; BNP=b-type natriuretic peptide; ECW=extracellular water; E/e' ratio=ratio of mitral inflow velocity to lateral annular relaxation velocity; eGFR=estimated glomerular filtration rate; ICW=intracellular water; IVC=inferior vena cava; LA=left atrial; LVEF=left ventricular ejection fraction; MAP=mean arterial pressure; MDRD=Modification of Diet in Renal Disease; PAP=pulmonary arterial pressure; PCR=protein-to-creatinine ratio; PCWP=pulmonary capillary wedge pressure; PVR=pulmonary vascular resistance; RA=right atrial; RAP=right atrial pressure; RRI=renal resistive index; RV=right ventricular; RV S'=systolic annular tissue velocity of the lateral tricuspid annulus; RVSI=renal venous stasis index; TAPSE=tricuspid annular plane systolic excursion.

Table S6. Correlation of renal function with relevant parameters*.

	Serum creatinine	p value†	eGFR (CKD-EPI creatinine-cystatin C equation)	p value†
	Correlation coefficient		Correlation coefficient	
Demographics				
Age, yrs	0.342	<0.0001	−0.542	<0.0001
Baseline clinical data				
PaO ₂ ‡	−0.021	0.764	0.028	0.685
PaCO ₂ ‡	0.005	0.944	0.053	0.451
6MWD	−0.211	0.0023	0.350	<0.0001
Laboratory data				
Hemoglobin	−0.166	0.0173	0.258	0.0002
Uric acid	0.479	<0.0001	−0.510	<0.0001
C-reactive protein	0.213	0.0022	−0.282	<0.0001
Maintenance therapy				
Loop diuretic dose	0.482	<0.0001	−0.389	<0.0001
Hemodynamics				
RAP	0.293	<0.0001	−0.323	<0.0001
PCWP	0.265	<0.0001	−0.270	<0.0001
Mixed venous oxygen saturation	−0.249	<0.0001	0.312	<0.0001
Echocardiographic parameters				
TAPSE	−0.315	<0.0001	0.300	<0.0001
RV myocardial performance index (Tei index)	−0.011	0.901	0.062	0.092
RV S'	−0.176	0.012	0.126	0.073
TAPSE/Systolic PAP ratio	−0.168	0.016	0.258	<0.0001
RA area	0.342	<0.0001	−0.333	<0.0001
LA diameter	0.310	<0.0001	0.310	<0.0001
Renal function				
Renal filtration gradient	−0.279	<0.0001	0.283	<0.0001
Urine PCR	0.180	0.0099	−0.240	0.0005
Urine ACR	0.179	0.0104	−0.238	0.0006
Urine α 1MCR	0.397	<0.0001	−0.523	<0.0001
Renal Doppler Ultrasonography				
RRI	0.237	<0.0001	−0.430	<0.0001
RVSI	0.486	<0.0001	−0.433	<0.0001
Neurohormonal status				
BNP	0.343	<0.0001	−0.416	<0.0001
Copeptin	0.554	<0.0001	−0.599	<0.0001
Urine FeNa	0.447	<0.0001	−0.492	<0.0001
Hydration status				
ECW/ICW ratio	0.085	0.246	−0.261	0.0003
Intra-abdominal pressure measurement				
Intra-abdominal pressure	0.333	<0.0001	−0.327	<0.0001

Pearson or Spearman correlation was considered as appropriate. *All available study variables were included in the analysis, but only variables that were significant in the analysis are presented here; in addition, paO₂ and paCO₂ are presented based on their clinical role. †After application of the Bonferroni correction, p<0.0006 was considered significant. ‡Blood gas measurements were taken from arterialized capillary ear lobe blood during right heart catheterization. In patients with long-term oxygen treatment, oxygen was applied via nasal cannula at the previously prescribed flow rate.

6MWD=6-min walk distance; ACR=albumin-to-creatinine ratio; α 1MCR= α 1-microglobulin-to-creatinine ratio; BNP=b-type natriuretic peptide; CKD-EPI=Chronic Kidney Disease Epidemiology Collaboration; ECW=extracellular water; E/e' ratio=ratio of mitral inflow velocity to lateral annular relaxation velocity; eGFR=estimated glomerular filtration rate; FeNa=fractional excretion of sodium; ICW=intracellular water; LA=left atrial; LVEF=left ventricular ejection fraction; MAP=mean arterial pressure; PaCO₂=arterial carbon dioxide pressure; PaO₂=arterial oxygen pressure; PAP=pulmonary arterial pressure; PCR=protein-to-creatinine

ratio; PCWP=pulmonary capillary wedge pressure; RA=right atrial; RAP=right atrial pressure; RV=right ventricular; RV S'=systolic annular tissue velocity of the lateral tricuspid annulus; RVSI=renal venous stasis index; TAPSE=tricuspid annular plane systolic excursion.

Table S7. Clinical characteristics, invasive hemodynamics, echocardiographic data, renal function, and neurohormonal and hydration status according to PH groups

	No PH (n=40)	Group 1 PH (pulmonary arterial hypertension) (n=46)	Group 2 PH (PH due to left heart disease) (n=30)	Group 3 PH (PH due to lung disease and/or hypoxemia) (n=41)	Group 4 PH (chronic thromboembolic PH) (n=34)	Group 5 PH (PH with unclear multifactorial mechanisms) (n=14)	p value*
Baseline clinical data							
Oxygen supply, n (%)		27 (58.7)	13 (43.3)	35 (85.4)	17 (50.0)	14 (100)	<0.0001
6MWD, m	313.15±126.56	309.07±153.40	269.60±115.46	199.12±105.30	308.38±147.46	239.43±104.40	<0.0001
NYHA classification, n (%)							0.0054
1–2	10 (25)	17 (37.0)	5 (16.7)	3 (7.3)	8 (23.5)	1 (7.1)	
3–4	30 (75)	29 (63.0)	25 (83.3)	38 (92.7)	26 (76.5)	13 (92.9)	
Comorbidities, n (%)							
Hypertension	23 (57.5)	21 (45.7)	27 (90.0)	32 (78.0)	18 (52.9)	7 (50.0)	<0.0001
Diabetes mellitus	8 (20.0)	8 (17.4)	11 (36.7)	11 (26.8)	6 (17.6)	4 (28.6)	0.388
Atrial fibrillation	10 (25.0)	7 (15.2)	24 (80.0)	6 (14.6)	7 (20.6)	2 (14.3)	<0.0001
Maintenance therapy							
ACEi or ARB, n (%)	18 (45.0)	12 (26.1)	21 (70.0)	18 (43.9)	9 (26.5)	5 (35.7)	0.0027
Loop diuretic dose, mg/day	0.0 [0.0–35.0]	40.0 [0.0–65.0]	50.0 [20.0–90.0]	40.0 [0.0–50.0]	40.0 [0.0–80.0]	40.0 [0.0–80.0]	0.0017
Thiazide diuretic, n (%)	9 (22.5)	18 (39.1)	11 (36.7)	17 (41.5)	12 (35.3)	5 (35.7)	0.567
Aldosterone antagonist, n (%)	8 (20.0)	22 (47.8)	12 (40.0)	13 (31.7)	17 (50.0)	4 (28.6)	0.0562
Triamterene, n (%)	0 (0)	3 (6.5)	0 (0)	0 (0)	1 (2.9)	1 (7.1)	0.197
PH-specific therapy, n (%)							<0.0001
Treatment-naïve	40 (100)	10 (21.7)	21 (70.0)	22 (53.7)	18 (52.9)	5 (35.7)	
Monotherapy	0 (0)	14 (30.4)	9 (30)	11 (26.8)	10 (29.4)	5 (35.7)	
Dual therapy	0 (0)	14 (30.4)	0 (0)	6 (14.6)	4 (11.7)	4 (28.6)	
≥Triple therapy	0 (0)	8 (17.4)	0 (0)	2 (4.9)	2 (5.9)	0 (0)	
Hemodynamics							
Mean PAP, mm Hg	17.68±4.60	42.13±18.07	37.90±12.03	35.63±9.31	36.91±8.25	46.00±11.75	<0.0001
PVR, dyn.s/cm ⁵	151.5 [89.5–223.8]	547.5 [343.8–786.5]	315.5 [166.3–478.5]	486.0 [344.5–707.5]	454.5 [334.0–632.5]	519.5 [475.0–613.5]	<0.0001
RAP, mm Hg	2.75±4.74	5.24±5.61	9.97±6.08	5.29±5.55	5.53±5.05	8.93±5.44	<0.0001
Cardiac index, L/min/m ²	3.10±1.41	2.69±0.80	2.68±0.92	2.47±0.67	2.56±0.64	2.99±1.31	0.0533
PCWP, mm Hg	7.0 [4.0–10.0]	8.5 [5.0–11.3]	19.0 [12.8–24.3]	7.0 [4.5–10.0]	8.0 [5.0–11.3]	12.0 [8.5–15.3]	<0.0001
Mixed venous oxygen saturation, %	67.65±7.01	64.69±8.81	61.91±8.81	62.69±7.05	60.73±8.72	64.05±8.51	0.0083
Heart rate, beats/min	71.45±11.11	70.39±11.46	66.13±12.01	73.98±12.91	72.15±13.56	97.71±21.30	0.0306
MAP, mm Hg†	86.28±10.54	81.28±10.42	82.94±10.16	84.91±13.16	82.58±13.07	84.52±10.88	0.191

Echocardiographic parameters							
<i>Right heart</i>							
TAPSE, mm	21.45±4.83	20.22±4.25	18.07±4.09	19.07±4.02	19.82±3.55	20.86±2.77	0.0269
RV myocardial performance index (Tei index)	0.40±0.19	0.52±0.22	0.43±0.19	0.54±0.22	0.52±0.25	0.49±0.27	0.237
RV S', cm/s	12.40±3.88	11.76 ±3.71	10.62±3.37	10.71±3.13	11.91±3.27	12.79±3.30	0.112
TAPSE/Systolic PAP ratio	0.67±0.24	0.31±0.15	0.32±0.11	0.33±0.16	0.35±0.15	0.32±0.10	<0.0001
Tricuspid insufficiency							0.159
Mild	23 (57.5)	14 (30.4)	6 (20.0)	14 (34.1)	8 (23.5)	3 (21.4)	
Moderate	12 (30.0)	22 (47.8)	14 (46.7)	15 (36.6)	16 (47.1)	4 (28.6)	
Severe	5 (12.5)	10 (21.7)	10 (33.3)	12 (29.2)	10 (29.4)	7 (50)	
RA area, m ²	15.15±6.47	18.42±6.56	20.70±6.93	19.25±6.62	20.78±6.00	21.85±5.58	0.0009
RV diameter, mm	36.43±7.88	42.13±8.29	40.31±8.02	42.20±8.24	41.21±6.16	44.57±7.86	0.0031
IVC, cm	2.15±0.47	2.25±0.59	2.37±0.41	2.30±0.46	2.27±0.43	2.45±0.50	0.317
<i>Left heart</i>							
LVEF, %	60.0 [58.1–65.0]	60.5 [60.0–65.0]	60.0 [55.0–65.0]	60.0 [60.0–65.0]	60.0 [60.0–65.0]	60.0 [60.0–65.0]	0.161
LA diameter, mm	40.87±7.60	40.70±6.90	47.47±6.40	40.89±6.08	40.44±5.40	43.69±5.22	<0.0001
LVEDD, mm	47.78±5.09	44.40±5.96	49.20±4.81	44.39±5.48	45.79±5.60	44.00±3.49	<0.0001
E/e' ratio	11.69±4.64	11.03±2.83	20.44±6.03	13.30±4.91	11.57±4.48	11.68±3.61	<0.0001
Renal function							
Serum creatinine, mg/dL‡	0.91±0.45	1.04±0.43	1.23±0.50	0.99±0.43	0.99±0.42	0.78±0.25	0.0175
Cystatin C, mg/L	0.97 [0.76–1.21]	1.19 [0.93–1.50]	1.36 [1.10–1.98]	1.09 [0.94–1.73]	1.07 [0.88–1.52]	1.06 [0.98–1.22]	0.0032
Urea, mg/dL§	39.98±29.56	45.67±42.10	61.57±34.11	49.05±29.86	49.15±44.64	35.50±14.40	0.143
eGFR (CKD-EPI creatinine equation), mL/min/1.73 m ²	83.28±23.76	73.30±27.87	56.57±21.63	77.15±25.32	71.97±25.05	89.50±21.14	<0.0001
eGFR (CKD-EPI creatinine-cystatin C equation), mL/min/1.73 m ² #	80.60±27.39	67.46±27.24	50.77±20.19	69.30±26.56	66.91±26.29	78.07±19.50	<0.0001
Renal filtration gradient, mm Hg**	73.88±10.66	66.19±10.32	65.01±11.71	70.03±14.57	68.05±13.88	68.45±11.52	0.0288
Urine PCR, mg/g creatinine	54.3 [44.9–82.9]	57.0 [35.9–106.3]	57.7 [35.6–131.7]	70.5 [46.7–146.2]	50.2 [36.4–121.9]	64.1 [44.8–111.9]	0.443
Urine ACR, mg/g creatinine	11.6 [6.1–17.0]	9.2 [5.3–27.1]	12.1 [7.9–39.7]	11.5 [6.6–66.2]	11.7 [7.5–29.3]	16.0 [6.5–55.3]	0.442
Urine α1MCR, mg/g creatinine	9.8 [15.9–18.6]	8.7 [4.9–17.6]	15.3 [9.3–27.9]	13.1 [5.6–34.5]	11.2 [4.7–22.0]	7.6 [6.2–11.5]	0.071
Acanthocyturia, n (%)	1 (2.5)	5 (10.9)	0 (0)	1 (2.4)	0 (0)	0 (0)	0.057
Sterile leukocyturia, n (%)	0 (0)	0 (0)	0 (0)	0 (0)	1 (2.9)	1 (7.1)	0.135

Intrarenal Doppler Ultrasonography							
Congestion stage							<0.0001
0	27 (67.5)	10 (21.7)	1 (3.3)	1 (24.4)	9 (26.5)	2 (14.3)	
1	13 (32.5)	20 (43.5)	12 (40)	16 (39.0)	14 (41.2)	6 (42.9)	
2	0 (0)	11 (23.9)	7 (23.3)	10 (24.4)	9 (26.5)	4 (28.6)	
3	0 (0)	5 (10.9)	10 (33.3)	5 (12.2)	2 (5.9)	2 (14.3)	
Venous impedance index of 1.0	13 (32.5)	36 (78.3)	29 (96.7)	31 (75.6)	25 (73.5)	12 (85.7)	0.482
RVSI	0.0 [0.00–0.09]	0.13 [0.04–0.34]	0.27 [0.11–0.46]	0.09 [0.02–0.29]	0.12 [0.00–0.29]	0.15 [0.06–0.36]	<0.0001
RRI	0.67±0.05	0.71±0.07	0.76±0.06	0.71±0.08	0.73±0.07	0.71±0.07	<0.0001
Neurohormonal status							
BNP, pg/mL	51.00 [22.5–175.5]	134.00 [375.5–324.8]	232.50 [157.5–590.0]	114.00 [55.0–538.5]	160.00 [98.5–314.5]	196.00 [45.8–531.0]	<0.0001
Copeptin, pmol/L	6.95 [4.2–13.5]	7.95 [5.2–18.9]	15.45 [6.4–39.2]	14.15 [8.0–27.7]	16.30 [6.8–23.1]	11.35 [6.1–20.1]	0.0063
Urine FeNa, %	0.60 [0.4–1.1]	0.65 [0.3–1.4]	1.20 [0.6–1.9]	0.80 [0.4–1.3]	0.50 [0.3–1.4]	0.4 [0.3–0.5]	0.0162
Sodium, mmol/L	139.33±3.24	139.24±3.14	139.90±2.90	139.66±3.03	139.47±3.52	140.50±1.51	0.783
BUN-to-creatinine ratio	20.28±8.18	19.09±6.80	23.05±7.86	22.58±7.22	21.47±7.84	21.29±6.46	0.189
Aldosterone, ng/dL	4.70 [3.00–8.45]	8.85 [3.90–19.88]	5.75 [3.00–10.90]	4.70 [3.00–12.30]	6.30 [3.00–11.83]	4.65 [3.00–6.95]	0.079
Potassium, mmol/L	3.75±0.45	3.61±0.39	3.78±0.45	3.60±0.43	3.62±0.40	3.67±0.25	0.271
Urine Na/K ratio	3.52±2.31	2.80±1.70	3.61±2.65	3.45±2.54	3.04±2.16	2.90±1.94	0.53
Hydration status							
Ascites, n (%)	0 (0)	2 (4.3)	3 (10.0)	1 (2.4)	1 (2.9)	0 (0)	0.588
Peripheral edema, n (%)	9 (22.5)	14 (30.4)	9 (30.0)	12 (29.3)	11 (32.4)	5 (35.7)	0.929
Pleural effusion, n (%)	0 (0)	5 (10.9)	3 (10.0)	3 (7.3)	2 (5.9)	4 (28.6)	0.0346
Hydration status (as measured by bioimpedance), L	0.11±1.64	0.97±2.02	1.05±2.53	0.54±2.21	0.71±2.28	1.35±1.91	0.282
Total body water, L	38.46±7.26	36.13±7.81	37.73±6.31	38.85±8.35	37.76±7.91	38.16±5.58	0.679
ECW, L	17.57±3.30	16.88±3.28	17.74±2.84	17.82±3.75	17.54±3.45	18.39±2.68	0.710
ICW, L	20.88±4.31	19.51±4.53	19.97±4.01	20.03±5.12	20.22±4.93	19.76±3.37	0.669
ECW/ICW ratio	0.85±0.09	0.87±0.12	0.90±0.12	0.86±0.13	0.88±0.13	0.94±0.11	0.132
Intra-abdominal pressure measurement							
Intra-abdominal pressure, mm Hg	6.0 [5.0–7.0]	7.0 [6.0–9.0]	8.5 [7.0–10.0]	7.0 [6.0–9.0]	7.0 [6.0–8.3]	8.0 [6.8–10.3]	<0.0001
Abdominal perfusion pressure, mm Hg††	80.08±10.50	73.73±10.11	75.99±10.66	79.47±13.70	75.31±13.35	74.74±10.95	0.092

Values are mean±SD, median [interquartile range], or n (%).

*After application of the Bonferroni correction, $p < 0.0008$ was considered significant. †MAP was calculated as (systolic blood pressure + 2x diastolic pressure)/3. ‡To convert the values for serum creatinine to $\mu\text{mol/L}$, multiply by 88.4. §To convert the values for urea to BUN, multiply by 0.467. ||eGFR was calculated with the CKD-EPI equation based on serum creatinine.²³ #eGFR was calculated with the CKD-EPI equation based on serum creatinine and cystatin C.²² **The renal filtration gradient was calculated as: MAP – 2x intra-abdominal pressure.²⁴ ††The abdominal perfusion pressure was calculated using the equation: MAP – intra-abdominal pressure.²⁴

6MWD=6-min walk distance; ACEi=angiotensin-converting enzyme inhibitor; ACR=albumin-to-creatinine ratio; $\alpha 1$ MCR= $\alpha 1$ -microglobulin-to-creatinine ratio; ARB=angiotensin receptor blocker; BNP=b-type natriuretic peptide; BUN=blood urea nitrogen; CKD-EPI=Chronic Kidney Disease Epidemiology Collaboration; ECW=extracellular water; E/e' ratio=ratio of mitral inflow velocity to lateral annular relaxation velocity; eGFR=estimated glomerular filtration rate; FeNa=fractional excretion of sodium; ICW=intracellular water; IVC=inferior vena cava; LA=left atrial; LVEDD=left ventricular end-diastolic diameter; LVEF=left ventricular ejection fraction; MAP=mean arterial pressure; Na/K=sodium/potassium; NYHA=New York Heart Association; PAP=pulmonary arterial pressure; PCR=protein-to-creatinine ratio; PCWP=pulmonary capillary wedge pressure; PH=pulmonary hypertension; PVR=pulmonary vascular resistance; RA=right atrial; RAP=right atrial pressure; RRI=renal resistive index; RV=right ventricular; RV S'=systolic annular tissue velocity of the lateral tricuspid annulus; RVSI=renal venous stasis index; TAPSE=tricuspid annular plane systolic excursion.

Table S8. Outcomes in the RHC cohort.

Outcome, n (%)	RHC cohort (n=205)
PH-related morbidity and death from any cause	91 (44.4%)
Unscheduled hospitalizations for fluid overload	64 (31.2%)
Escalations of PH-specific therapy	71 (34.6%)
Death from any cause	21 (10.2%)

Five patients underwent pulmonary thrombendarterectomy, and one patient underwent lung transplantation.

RHC=right heart catheterization; PH=pulmonary hypertension.

Table S9. Predictors of morbidity and mortality by the univariate Cox proportional hazard model.

Predictor	Univariate	
	HR (95% CI)	p value
Baseline clinical data		
Age	1.02 (1.00–1.03)	0.0439
Sex	0.63 (0.42–0.95)	0.0265
6MWD	0.997 (0.996–0.999)	0.0006
NYHA classification	1.62 (1.19–2.20)	0.0024
Pulmonary hypertension group	0.81 (0.72–0.91)	<0.0001
Diabetes mellitus	1.88 (1.21–2.91)	0.0048
Atrial fibrillation	2.56 (1.68–3.88)	<0.0001
Uric acid	1.25 (1.16–1.34)	<0.0001
Hemodynamics		
Mean PAP	1.03 (1.02–1.04)	<0.0001
PVR	1.00 (1.00–1.00)	<0.0001
RAP	1.12 (1.07–1.14)	<0.0001
Cardiac index	0.54 (0.39–0.74)	<0.0001
PCWP	1.06 (1.03–1.09)	<0.0001
Mixed venous oxygen saturation	0.93 (0.91–0.96)	<0.0001
Echocardiographic parameters		
TAPSE	0.90 (0.86–0.94)	<0.0001
RV S'	0.86 (0.80–0.93)	<0.0001
TAPSE/Systolic PAP ratio	0.05 (0.01–0.19)	<0.0001
Tricuspid insufficiency	1.76 (1.32–2.35)	<0.0001
RA area	1.07 (1.04–1.09)	<0.0001
RV diameter	1.05 (1.02–1.07)	<0.0001
IVC diameter	2.08 (1.38–3.13)	<0.0001
LVEF	0.98 (0.95–1.00)	0.0477
LA diameter	1.07 (1.04–1.10)	<0.0001
E/e' ratio	1.07 (1.03–1.11)	<0.0001
Renal function		
Serum creatinine	2.59 (1.83–3.66)	<0.0001
Cystatin C	2.18 (1.69–2.82)	<0.0001
Urea	1.01 (1.01–1.02)	<0.0001
eGFR (MDRD equation)*	0.99 (0.98–0.99)	<0.0001
eGFR (CKD-EPI creatinine equation) †	0.98 (0.97–0.98)	<0.0001
eGFR (CKD-EPI creatinine-cystatin C equation)‡	0.98 (0.97–0.99)	<0.0001
Renal filtration gradient	0.97 (0.95–0.99)	0.0007
Urine α 1MCR	1.01 (1.01–1.02)	<0.0001
Urine FeNa	1.21 (1.09–1.34)	<0.0001
Renal Doppler ultrasonography		
RVSI tertiles	20.57 (9.03–46.87)	<0.0001
1 st tertile RVSI group vs RVSI=0	2.31 (1.06–5.05)	0.0363
2 nd tertile RVSI group vs RVSI=0	3.63 (1.71–7.65)	0.0007
3 rd tertile RVSI group vs RVSI=0	8.70 (4.33–17.48)	<0.0001
Congestion stages	2.00 (1.63–2.44)	<0.0001
Stage 1 congestion vs stage 0	2.65 (1.29–5.44)	0.0078
Stage 2 congestion vs stage 0	6.35 (3.08–13.09)	<0.0001
Stage 3 congestion vs stage 0	8.45 (3.98–17.96)	<0.0001
Venous impedance index	14.61 (4.31–49.55)	<0.0001
Neurohormonal status		
BNP	1.00 (1.00–1.00)	<0.0001
Copeptin	1.02 (1.02–1.03)	<0.0001
Aldosterone	1.01 (1.00–1.02)	0.0184
Hydration status		
Hydration status (as measured by bioimpedance)	1.14 (1.03–1.25)	0.0081
Extracellular/intracellular water	8.42 (1.31–54.25)	0.0251
Ascites	2.85 (1.30–6.23)	0.0089
Pleural effusion	2.27 (1.26–4.10)	0.0064
Intra-abdominal pressure measurement		
Intra-abdominal pressure	1.25 (1.17–1.34)	<0.0001
Abdominal perfusion pressure§	0.98 (0.96–1.00)	0.0226

All available study variables were included in the univariate analysis, but only variables that were significant in the univariate analysis are presented here. *eGFR was calculated with the MDRD equation based on serum creatinine.²⁵ †eGFR was calculated with the CKD-EPI equation based on serum creatinine.²³ ‡eGFR was calculated with the CKD-EPI equation based on serum creatinine and cystatin C.²² §The abdominal perfusion pressure was calculated using the equation: MAP–intra-abdominal pressure, while MAP was calculated as (systolic blood pressure+2x diastolic pressure)/3.²⁴

6MWD=6-min walk distance; α 1MCR= α 1-microglobulin-to-creatinine ratio; BNP=b-type natriuretic peptide; CKD-EPI=Chronic Kidney Disease Epidemiology Collaboration; CI=confidence interval; E/e' ratio=ratio of

mitral inflow velocity to lateral annular relaxation velocity; eGFR=estimated glomerular filtration rate; FeNa=fractional excretion of sodium; HR=hazard ratio; IVC=inferior vena cava; LA=left atrial; LVEF=left ventricular ejection fraction; MAP=mean arterial pressure; MDRD=Modification of Diet in Renal Disease; NYHA=New York Heart Association; PAP=pulmonary arterial pressure; PCWP=pulmonary capillary wedge pressure; PVR=pulmonary vascular resistance; RA=right atrial; RAP=right atrial pressure; RV=right ventricular; RV S'=systolic annular tissue velocity of the lateral tricuspid annulus; RVSI=renal venous stasis index; TAPSE=tricuspid annular plane systolic excursion.

Table S10. Predictors of unscheduled hospitalization due to fluid overload by the univariate Cox proportional hazard model.

Predictor	Univariate	
	HR (95% CI)	p value
Baseline clinical data		
Age	1.04 (1.01–1.06)	0.0013
Sex	0.48 (0.29–0.79)	0.0039
6MWD	0.996 (0.994–0.998)	<0.0001
NYHA classification	1.81 (1.24–2.64)	0.0022
Pulmonary hypertension group	0.83 (0.72–0.95)	0.0083
Diabetes mellitus	2.58 (1.56–4.27)	<0.0001
Atrial fibrillation	4.05 (2.47–6.63)	<0.0001
Sodium	0.93 (0.86–0.99)	0.0286
Uric acid	1.29 (1.19–1.41)	<0.0001
Hemodynamics		
Mean PAP	1.02 (1.01–1.04)	0.0008
PVR	1.00 (1.00–1.00)	0.0246
RAP	1.15 (1.11–1.20)	<0.0001
Cardiac index	0.46 (0.31–0.68)	<0.0001
PCWP	1.08 (1.05–1.11)	<0.0001
Mixed venous oxygen saturation	0.92 (0.90–0.95)	<0.0001
Echocardiographic parameters		
TAPSE	0.86 (0.81–0.91)	<0.0001
RV S'	0.77 (0.70–0.85)	<0.0001
TAPSE/Systolic PAP ratio	0.02 (0.00–0.18)	<0.0001
Tricuspid insufficiency	2.22 (1.55–3.18)	<0.0001
RA area	1.11 (1.07–1.14)	<0.0001
RV diameter	1.06 (1.03–1.10)	<0.0001
IVC diameter	2.60 (1.59–4.16)	<0.0001
LVEF	0.96 (0.94–0.99)	0.0037
LA diameter	1.07 (1.04–1.11)	<0.0001
E/e' ratio	1.08 (1.03–1.12)	<0.0001
Renal function		
Serum creatinine	3.40 (2.33–4.94)	<0.0001
Cystatin C	2.62 (1.99–3.45)	<0.0001
Urea	1.01 (1.01–1.02)	<0.0001
eGFR (MDRD equation)*	0.98 (0.97–0.99)	<0.0001
eGFR (CKD-EPI creatinine equation) †	0.97 (0.96–0.98)	<0.0001
eGFR (CKD-EPI creatinine-cystatin C equation)‡	0.97 (0.96–0.98)	<0.0001
BUN-to-creatinine ratio	1.04 (1.01–1.07)	0.0117
Renal filtration gradient	0.96 (0.94–0.98)	<0.0001
Urine α 1MCR	1.01 (1.01–1.02)	<0.0001
Urine FeNa	1.21 (1.07–1.36)	0.0017
Renal Doppler ultrasonography		
RVSI tertiles	1.71 (1.48–1.98)	<0.0001
1 st tertile RVSI group vs RVSI=0	6.49 (1.42–29.64)	0.0157
2 nd tertile RVSI group vs RVSI=0	10.98 (2.52–47.76)	0.0014
3 rd tertile RVSI group vs RVSI=0	35.60 (8.54–148.38)	<0.0001
Congestion stages	2.49 (1.94–3.20)	<0.0001
Stage 1 congestion vs stage 0	7.36 (1.71–31.72)	0.0074
Stage 2 congestion vs stage 0	25.51 (6.05–107.67)	<0.0001
Stage 3 congestion vs stage 0	32.17 (7.44–139.09)	<0.0001
Venous impedance index	121.10 (9.45–1552.61)	<0.0001
Neurohormonal status		
BNP	1.00 (1.00–1.00)	<0.0001
Copeptin	1.03 (1.02–1.04)	<0.0001
Aldosterone	1.02 (1.00–1.03)	0.0122
Hydration status		
Hydration status (as measured by bioimpedance)	1.16 (1.04–1.29)	0.0089
Extracellular/intracellular water	14.97 (1.66–135.09)	0.0159
Extracellular water	1.09 (1.01–1.18)	0.0280
Ascites	3.11 (1.24–7.77)	0.0153
Pleural effusion	2.42 (1.19–4.90)	0.0142
Peripheral edema	2.09 (1.28–3.44)	0.0034
Intra-abdominal pressure measurement		
Intra-abdominal pressure	1.36 (1.26–1.47)	<0.0001
Abdominal perfusion pressure§	0.97 (0.95–1.00)	0.0210

All available study variables were included in the univariate analysis, but only variables that were significant in the univariate analysis are presented here. *eGFR was calculated with the MDRD equation based on serum creatinine.²⁵ †eGFR was calculated with the CKD-EPI equation based on serum creatinine.²³ ‡eGFR was calculated with the CKD-EPI equation based on serum creatinine and cystatin C.²² §The abdominal perfusion

pressure was calculated using the equation: $\text{MAP} = \text{intra-abdominal pressure} + \frac{\text{systolic blood pressure} - \text{diastolic blood pressure}}{3}$, while MAP was calculated as (systolic blood pressure+2x diastolic pressure)/3.²⁴

6MWD=6-min walk distance; $\alpha 1\text{MCR} = \alpha 1\text{-microglobulin-to-creatinine ratio}$; BNP=b-type natriuretic peptide; BUN=blood urea nitrogen; CKD-EPI=Chronic Kidney Disease Epidemiology Collaboration; CI=confidence interval; E/e' ratio=ratio of mitral inflow velocity to lateral annular relaxation velocity; eGFR=estimated glomerular filtration rate; FeNa=fractional excretion of sodium; IVC=inferior vena cava; HR=hazard ratio; LA=left atrial; LVEF=left ventricular ejection fraction; MAP=mean arterial pressure; MDRD=Modification of Diet in Renal Disease; NYHA=New York Heart Association; PAP=pulmonary arterial pressure; PCR=protein-to-creatinine ratio; PCWP=pulmonary capillary wedge pressure; PVR=pulmonary vascular resistance; RA=right atrial; RAP = right atrial pressure; RV=right ventricular; RV S'=systolic annular tissue velocity of the lateral tricuspid annulus; RVSI=renal venous stasis index; TAPSE=tricuspid annular plane systolic excursion.

Table S11. Predictors of escalation of PH-specific therapy by the univariate Cox proportional hazard model.

Predictor	Univariate	
	HR (95% CI)	p value
Baseline clinical data		
6MWD	0.997 (0.995–0.999)	0.0013
NYHA classification	1.59 (1.11–2.27)	0.0110
Pulmonary hypertension group	0.79 (0.69–0.91)	0.0008
Diabetes mellitus	1.90 (1.16–3.12)	0.0105
Atrial fibrillation	1.79 (1.11–2.89)	0.0177
Potassium	0.49 (0.28–0.88)	0.0162
Uric acid	1.26 (1.16–1.36)	<0.0001
Hemodynamics		
Mean PAP	1.03 (1.02–1.04)	<0.0001
PVR	1.00 (1.00–1.00)	<0.0001
RAP	1.08 (1.04–1.12)	<0.0001
Cardiac index	0.41 (0.28–0.60)	<0.0001
PCWP	1.04 (1.01–1.07)	0.0072
Mixed venous oxygen saturation	0.92 (0.90–0.95)	<0.0001
Echocardiographic parameters		
TAPSE	0.89 (0.85–0.94)	<0.0001
RV S'	0.84 (0.77–0.91)	<0.0001
TAPSE/Systolic PAP ratio	0.04 (0.01–0.21)	<0.0001
Tricuspid insufficiency	1.54 (1.12–2.12)	0.0079
RA area	1.05 (1.02–1.09)	0.0013
RV diameter	1.05 (1.02–1.08)	0.0005
IVC diameter	2.00 (1.25–3.19)	0.0037
LA diameter	1.05 (1.01–1.08)	0.0072
LVEDD	0.95 (0.91–0.99)	0.0221
E/e' ratio	1.07 (1.03–1.12)	0.0006
Renal function		
Serum creatinine	2.55 (1.74–3.73)	<0.0001
Urea	1.01 (1.00–1.01)	<0.0001
Cystatin C	1.95 (1.50–2.55)	<0.0001
eGFR (MDRD equation)*	0.99 (0.98–0.99)	<0.0001
eGFR (CKD-EPI creatinine equation) †	0.98 (0.97–0.99)	<0.0001
eGFR (CKD-EPI creatinine-cystatin C equation)‡	0.98 (0.97–0.99)	<0.0001
Renal filtration gradient	0.96 (0.94–0.99)	0.0007
Urine α 1MCR	1.01 (1.01–1.02)	<0.0001
Urine FeNa	1.24 (1.10–1.39)	<0.0001
Renal Doppler ultrasonography		
RVSI tertiles	1.43 (1.26–1.63)	<0.0001
1 st tertile RVSI group vs RVSI=0	2.16 (0.89–5.24)	0.0872
2 nd tertile RVSI group vs RVSI=0	3.52 (1.53–8.07)	0.0030
3 rd tertile RVSI group vs RVSI=0	7.03 (3.22–15.35)	<0.0001
Congestion stages	1.86 (1.49–2.33)	<0.0001
Stage 1 congestion vs stage 0	2.37 (1.05–5.35)	0.0373
Stage 2 congestion vs stage 0	6.22 (2.79–13.87)	<0.0001
Stage 3 congestion vs stage 0	6.39 (2.73–14.97)	<0.0001
Venous impedance index	12.59 (3.20–49.45)	<0.0001
Neurohormonal status		
BNP	1.00 (1.00–1.00)	<0.0001
Copeptin	1.03 (1.02–1.04)	<0.0001
Hydration status		
Pleural effusion	2.15 (1.10–4.21)	0.0256
Intra-abdominal pressure measurement		
Intra-abdominal pressure	1.22 (1.13–1.32)	<0.0001
Abdominal perfusion pressure§	0.97 (0.95–0.99)	0.0098

All available study variables were included in the univariate analysis, but only variables that were significant in the univariate analysis are presented here. *eGFR was calculated with the MDRD equation based on serum creatinine.²⁵ †eGFR was calculated with the CKD-EPI equation based on serum creatinine.²³ ‡eGFR was calculated with the CKD-EPI equation based on serum creatinine and cystatin C.²² §The abdominal perfusion pressure was calculated using the equation: MAP–intra-abdominal pressure, while MAP was calculated as (systolic blood pressure+2x diastolic pressure)/3.²⁴

6MWD=6-min walk distance; α 1MCR= α 1-microglobulin-to-creatinine ratio; BNP=b-type natriuretic peptide; CKD-EPI=Chronic Kidney Disease Epidemiology Collaboration; CI=confidence interval; E/e' ratio=ratio of mitral inflow velocity to lateral annular relaxation velocity; eGFR=estimated glomerular filtration rate; FeNa=fractional excretion of sodium; HR=hazard ratio; IVC=inferior vena cava; LA=left atrial; LVEDD=left ventricular end-diastolic diameter; MAP=mean arterial pressure; MDRD=Modification of Diet in Renal Disease;

NYHA=New York Heart Association; PAP=pulmonary arterial pressure; PCWP=pulmonary capillary wedge pressure; PH=pulmonary hypertension; PVR=pulmonary vascular resistance; RA=right atrial; RAP=right atrial pressure; RV=right ventricular; RV S'=systolic annular tissue velocity of the lateral tricuspid annulus; RVSI=renal venous stasis index; TAPSE=tricuspid annular plane systolic excursion.

Table S12. Predictors of death from any cause by the univariate Cox proportional hazard model.

Predictor	Univariate	
	HR (95% CI)	p value
Baseline clinical data		
Sex	0.30 (0.12–0.77)	0.0127
6MWD	1.0 (0.99–1.00)	0.0239
NYHA classification	2.65 (1.30–5.41)	0.0074
Uric acid	1.25 (1.09–1.43)	0.0018
Hemodynamics		
RAP	1.08 (1.02–1.15)	0.0149
Mixed venous oxygen saturation	0.92 (0.88–0.96)	<0.0001
Echocardiographic parameters		
TAPSE	0.88 (0.80–0.96)	0.0045
RV S'	0.74 (0.64–0.87)	<0.0001
TAPSE/Systolic PAP ratio	0.01 (0.00–0.17)	0.011
RA area	1.10 (1.04–1.17)	0.0018
RV diameter	1.07 (1.02–1.12)	0.0076
Renal function		
Serum creatinine	2.14 (1.05–4.40)	0.0376
Urea	1.01 (1.00–1.02)	0.0262
Renal Doppler ultrasonography		
RVSI tertiles		0.065
1 st tertile RVSI group vs RVSI=0	2.00 (0.48–8.38)	0.342
2 nd tertile RVSI group vs RVSI=0	1.25 (0.25–6.17)	0.788
3 rd tertile RVSI group vs RVSI=0	4.33 (1.19–15.72)	0.026
Congestion stages	1.39 (1.10–1.77)	0.0066
Stage 1 congestion vs stage 0	1.29 (0.31–5.38)	0.732
Stage 2 congestion vs stage 0	3.84 (1.02–14.48)	0.0469
Stage 3 congestion vs stage 0	4.03 (0.96–16.86)	0.0564
Neurohormonal status		
BNP	1.00 (1.00–1.00)	0.0012
Copeptin	1.02 (1.00–1.04)	0.0193
Intra-abdominal pressure measurement		
Intra-abdominal pressure	1.22 (1.06–1.41)	0.0069

All available study variables were included in the univariate analysis, but only variables that were significant in the univariate analysis are presented here.

6MWD=6-min walk distance; BNP=b-type natriuretic peptide; CI=confidence interval; HR=hazard ratio; NYHA=New York Heart Association; PAP=pulmonary arterial pressure; RA=right atrial; RAP=right atrial pressure; RV=right ventricular; RV S'=systolic annular tissue velocity of the lateral tricuspid annulus; RVSI=renal venous stasis index; TAPSE=tricuspid annular plane systolic excursion.

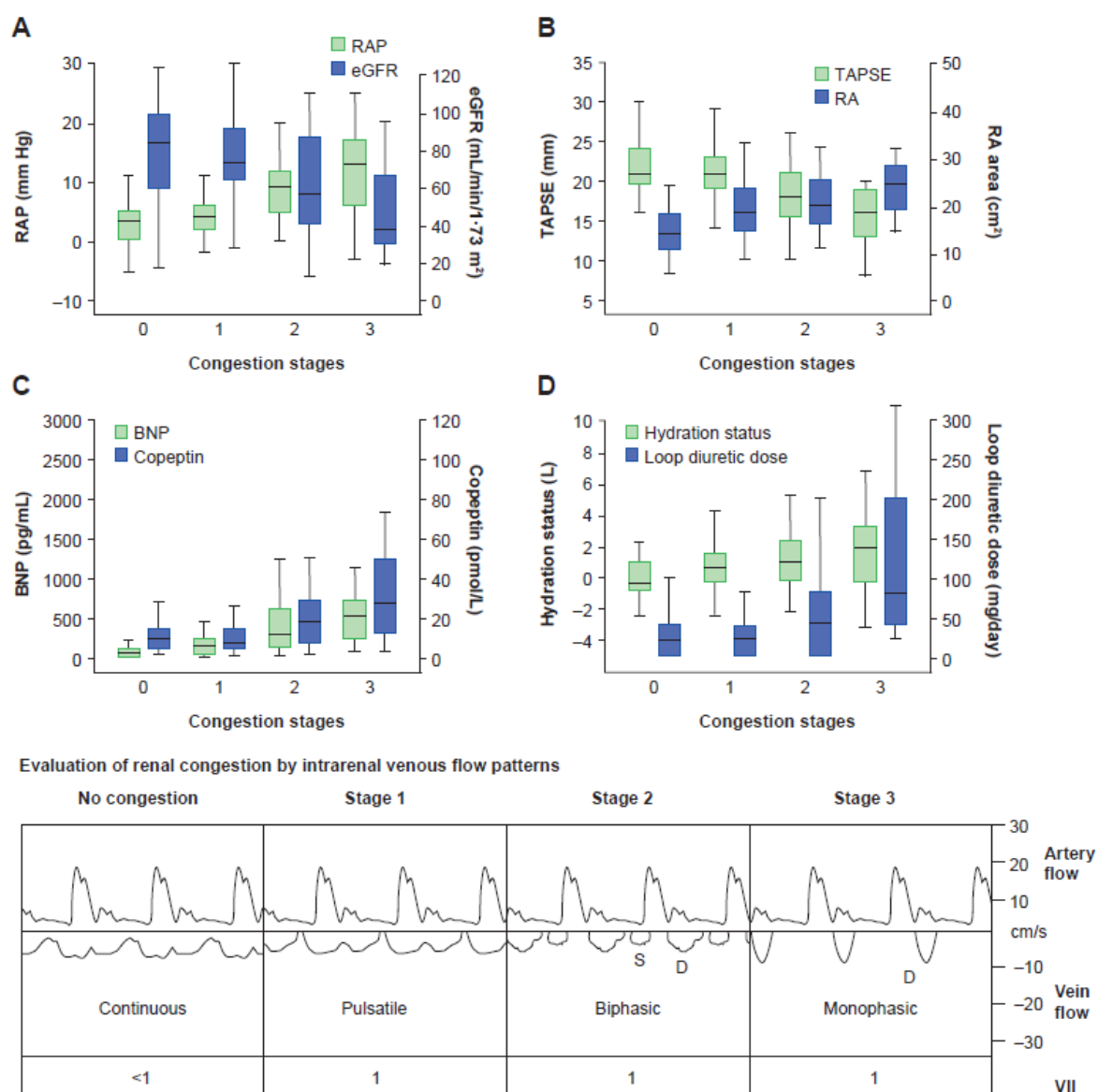
Table S13. Performance of RVSI versus IRVF patterns in models including both variables for prediction of secondary endpoints.

Secondary endpoint	Wald statistic		
	Unplanned hospitalization due to fluid overload	Escalation of PH-specific therapy	All-cause mortality
RVSI	6.163	0.721	0.611
IRVF patterns	0.996	2.675	0.204

Higher Wald statistic indicates superiority for prediction of endpoint. RVSI was superior to IRVF patterns in models including both RVSI and IRVF patterns as predictor variables for all component endpoints except need for escalation of PH-specific therapy.

IRVF=intrarenal venous flow; PH=pulmonary hypertension; RVSI=renal venous stasis index.

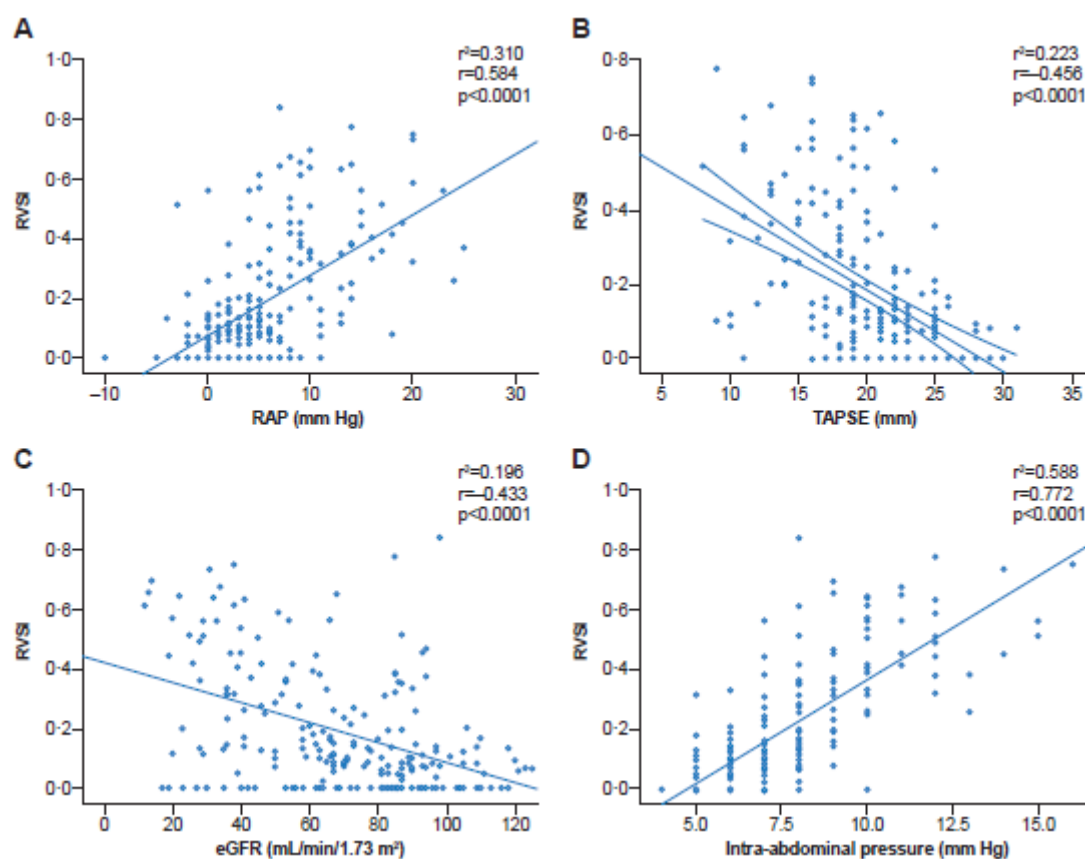
Figure S1. IRVF patterns and associated clinical parameters.



Severity of renal congestion can be evaluated by identifying four distinct IRVF patterns using renal Doppler ultrasonography. The figure illustrates the associations of these IRVF patterns with RAP and renal function (a), right ventricular systolic function and right atrial area (b), neurohormonal (c), and hydration status (d). Fluid overload as measured by bioimpedance is likely to occur as a result of hemodynamic alterations and neurohormonal activation leading to a deterioration of renal function and fluid retention.

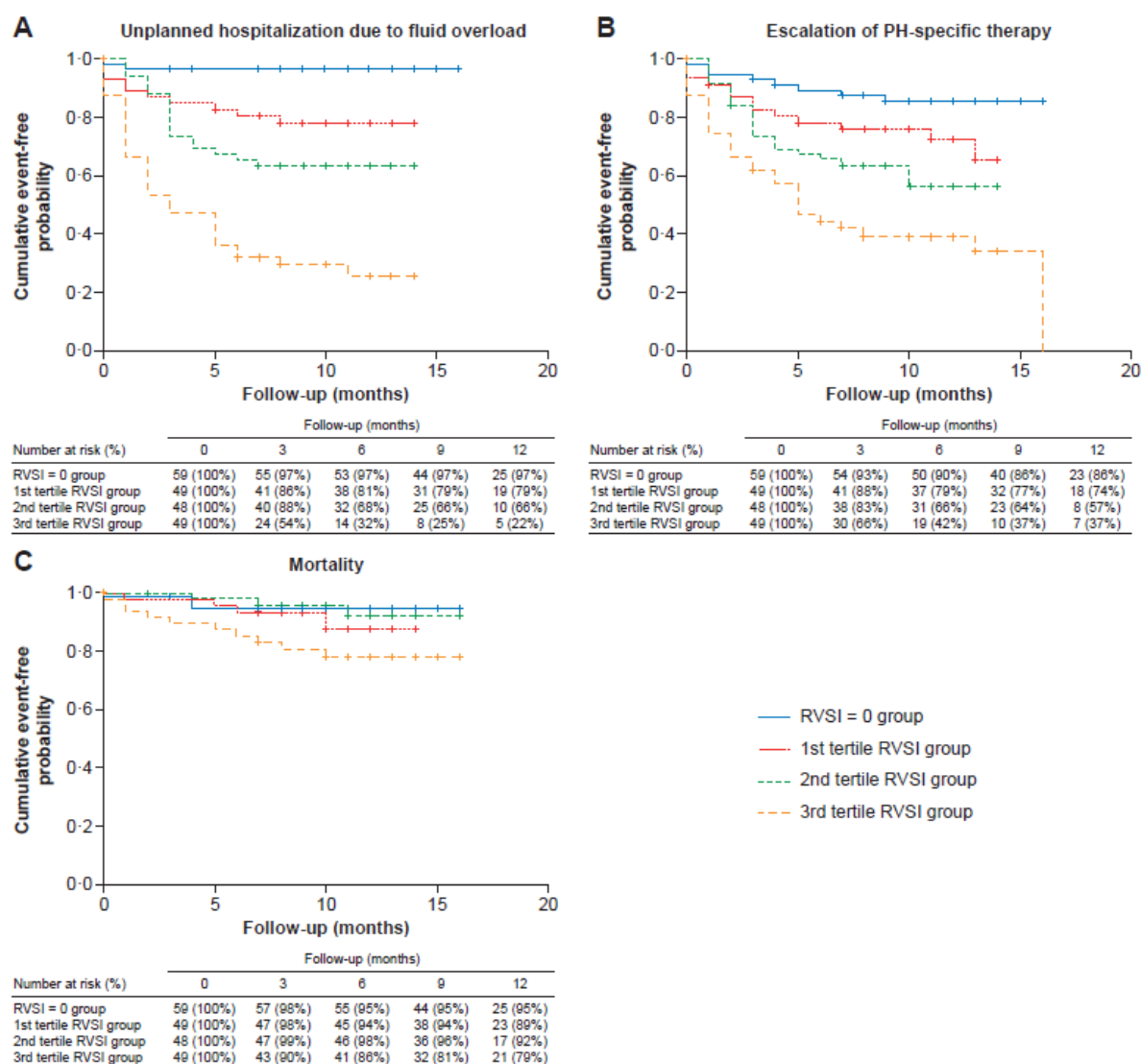
BNP=b-type natriuretic peptide; D=diastole; eGFR=estimated glomerular filtration rate (based on Chronic Kidney Disease Epidemiology Collaboration creatinine-cystatin C equation²²); IRVF=intrarenal venous flow; RA=right atrial; RAP=right atrial pressure; S=systole; TAPSE=tricuspid annular plane systolic excursion; VII=venous impedance index.

Figure S2. Correlation of RVSI with RAP (a), TAPSE (b), eGFR (c), and intra-abdominal pressure (d).



eGFR=estimated glomerular filtration rate (based on Chronic Kidney Disease Epidemiology Collaboration creatinine-cystatin C equation²²); RAP=right atrial pressure; RVSI=renal venous stasis index; TAPSE=tricuspid annular plane systolic excursion.

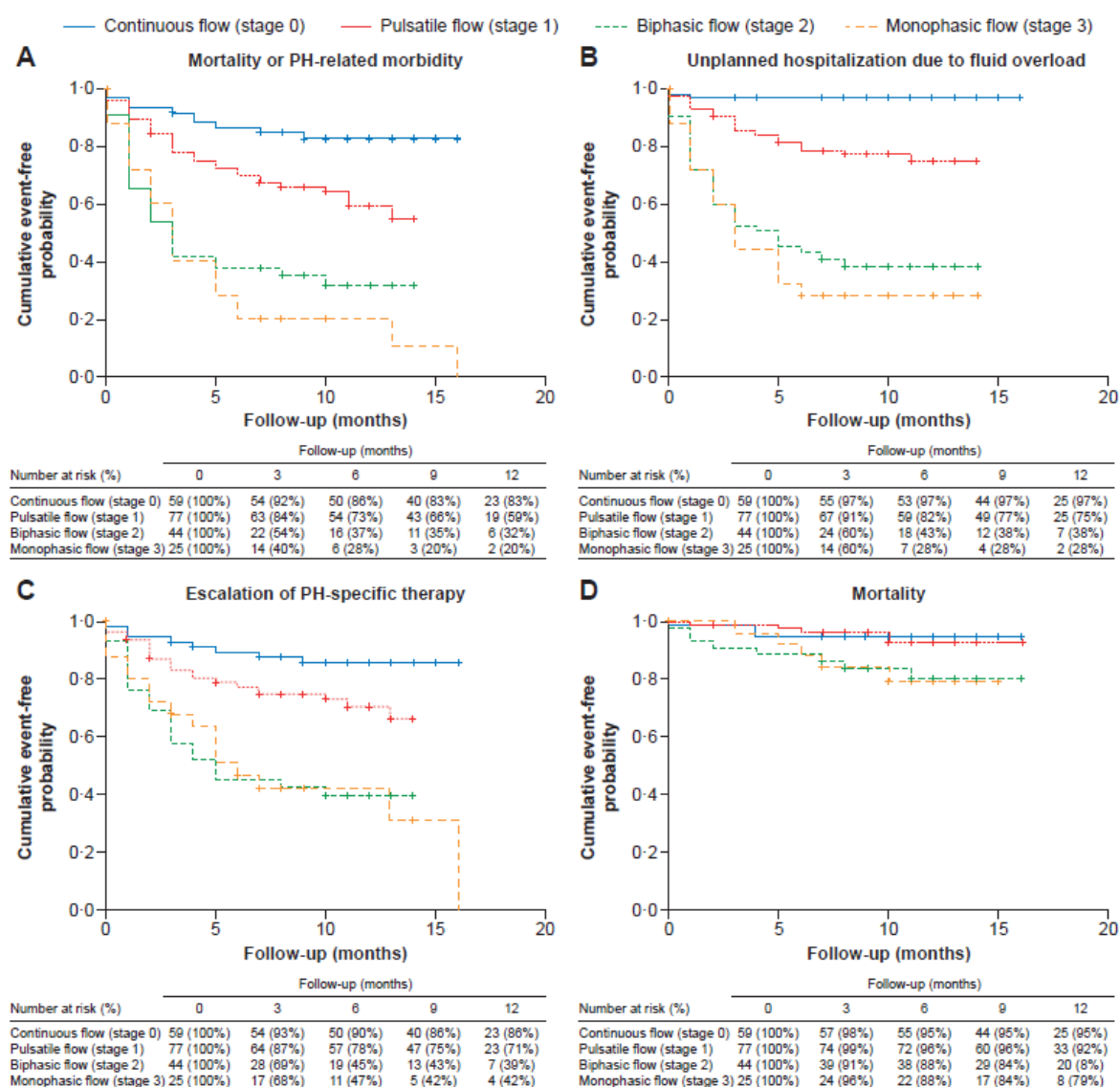
Figure S3. Kaplan-Meier estimate curves according to RVSI tertiles.



Patients in the 3rd tertile RVSI group had a significantly higher probability than other patients of the following individual components of the composite endpoint: unscheduled hospitalization for fluid overload ($p < 0.0001$) (**a**) and escalation of PH-specific therapy ($p < 0.0001$) (**b**). After Bonferroni correction, death from any cause did not show a significant difference between patients in the 3rd tertile RVSI group and other patients ($p = 0.0412$) (**c**).

PH=pulmonary hypertension; RVSI = renal venous stasis index.

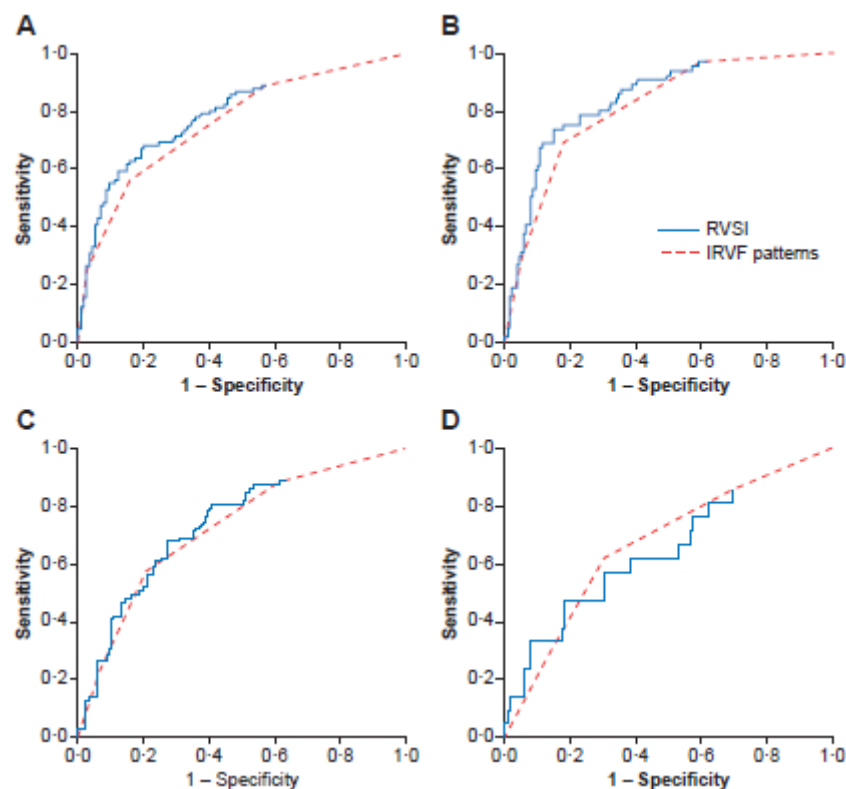
Figure S4. Kaplan-Meier estimate curves according to IRVF patterns.



Patients in the highest IRVF pattern group had a significantly higher probability than other patients of the composite endpoint of PH-related morbidity or death from any cause ($p < 0.0001$) (a) and the following individual components of the composite endpoint: unscheduled hospitalization for fluid overload ($p < 0.0001$) (b) and escalation of PH-specific therapy ($p < 0.0001$) (c). After Bonferroni correction, death from any cause did not show a significant difference between patients in the highest IRVF pattern group and other patients ($p = 0.0387$) (d).

IRVF=intrarenal venous flow; PH=pulmonary hypertension.

Figure S5. Comparison of RVSI and IRVF patterns as predictors of the primary and secondary clinical endpoints.



Receiver operating characteristic analyses indicate that RVSI was superior to the four IRVF patterns as a predictor of the composite primary endpoint (AUC: 0.789 and 0.761, respectively; $p=0.038$) **(a)**, and for the prediction of unplanned hospitalization due to fluid overload (AUC: 0.843 and 0.813, respectively; $p=0.045$) **(b)** but not escalation of pulmonary hypertension-specific therapy (AUC: 0.737 and 0.724, respectively; $p=0.36$) **(c)**, nor all-cause mortality (AUC: 0.650 and 0.668, respectively; $p=0.37$) **(d)**. Diagonal segments are produced by ties.

AUC=area under the curve; IRVF=intrarenal venous flow; RVSI=renal venous stasis index.

SUPPLEMENTAL REFERENCES:

1. Galie N, Humbert M, Vachiery JL, Gibbs S, Lang I, Torbicki A, Simonneau G, Peacock A, Vonk Noordegraaf A, Beghetti M, Ghofrani A, Gomez Sanchez MA, Hansmann G, Klepetko W, Lancellotti P, Matucci M, McDonagh T, Pierard LA, Trindade PT, Zompatori M, Hoeper M and Group ESCSD. 2015 ESC/ERS Guidelines for the diagnosis and treatment of pulmonary hypertension: The Joint Task Force for the Diagnosis and Treatment of Pulmonary Hypertension of the European Society of Cardiology (ESC) and the European Respiratory Society (ERS): Endorsed by: Association for European Paediatric and Congenital Cardiology (AEPC), International Society for Heart and Lung Transplantation (ISHLT). *Eur Heart J*. 2016; 37:67-119.
2. Kushner RF. Bioelectrical impedance analysis: a review of principles and applications. *J Am Coll Nutr*. 1992; 11:199-209.
3. McCullough PA and Brown JR. Effects of Intra-Arterial and Intravenous Iso-Osmolar Contrast Medium (Iodixanol) on the Risk of Contrast-Induced Acute Kidney Injury: A Meta-Analysis. *Cardiorenal Med*. 2011; 1:220-234.
4. Chamney PW, Wabel P, Moissl UM, Muller MJ, Bosy-Westphal A, Korth O and Fuller NJ. A whole-body model to distinguish excess fluid from the hydration of major body tissues. *Am J Clin Nutr*. 2007; 85:80-9.
5. Moissl UM, Wabel P, Chamney PW, Bosaeus I, Levin NW, Bosy-Westphal A, Korth O, Muller MJ, Ellegard L, Malmros V, Kaitwatcharachai C, Kuhlmann MK, Zhu F and Fuller NJ. Body fluid volume determination via body composition spectroscopy in health and disease. *Physiol Meas*. 2006; 27:921-33.
6. Passauer J, Petrov H, Schleser A, Leicht J and Pucalka K. Evaluation of clinical dry weight assessment in haemodialysis patients using bioimpedance spectroscopy: a cross-sectional study. *Nephrol Dial Transplant*. 2010;25: 545-51.
7. Marcelli D, Usvyat LA, Kotanko P, Bayh I, Canaud B, Etter M, Gatti E, Grassmann A, Wang Y, Marelli C, Scatizzi L, Stopper A, van der Sande FM, Kooman J and Consortium MODO. Body composition and survival in dialysis patients: results from an international cohort study. *Clin J Am Soc Nephrol*. 2015; 10:1192-200.
8. Valtuille R, Casos ME, Fernandez EA, Guinsburg A and Marelli C. Nutritional Markers and Body Composition in Hemodialysis Patients. *Int Sch Res Notices*. 2015; 2015:695263.
9. Buch E, Bradfield J, Larson T and Horwich T. Effect of bioimpedance body composition analysis on function of implanted cardiac devices. *Pacing Clin Electrophysiol*. 2012; 35:681-4.
10. Wabel P, Moissl U, Chamney P, Jirka T, Machek P, Ponce P, Taborsky P, Tetta C, Velasco N, Vlasak J, Zaluska W and Wizemann V. Towards improved cardiovascular management: the necessity of combining blood pressure and fluid overload. *Nephrol Dial Transplant*. 2008; 23:2965-71.
11. Wieskotten S, Heinke S, Wabel P, Moissl U, Becker J, Pirlich M, Keymeling M and Isermann R. Bioimpedance-based identification of malnutrition using fuzzy logic. *Physiol Meas*. 2008;29:639-54.
12. Ronco C, Verger C, Crepaldi C, Pham J, De Los Rios T, Gauly A, Wabel P, Van Biesen W and Group I-PS. Baseline hydration status in incident peritoneal dialysis patients: the initiative of patient outcomes in dialysis (I-POD-PD study) dagger. *Nephrol Dial Transplant*. 2015; 30:849-58.
13. Ponikowski P, Voors AA, Anker SD, Bueno H, Cleland JG, Coats AJ, Falk V, Gonzalez-Juanatey JR, Harjola VP, Jankowska EA, Jessup M, Linde C, Nihoyannopoulos P, Parissis JT, Pieske B, Riley JP, Rosano GM, Ruilope LM, Ruschitzka F, Rutten FH, van der Meer P and Authors/Task Force M. 2016 ESC Guidelines for the diagnosis and treatment of acute and chronic heart failure: The Task Force for the diagnosis and treatment of acute and chronic heart failure of the European Society of Cardiology (ESC). Developed with the special contribution of the Heart Failure Association (HFA) of the ESC. *Eur Heart J*. 2016; 37:2129-200.
14. Morgenthaler NG, Struck J, Alonso C and Bergmann A. Assay for the measurement of copeptin, a stable peptide derived from the precursor of vasopressin. *Clin Chem*. 2006; 52:112-9.
15. Cystatin C. CKD-EPI (Chronic Kidney Disease Epidemiology Collaboration). (Accessed 27 Oct, at <http://ckdepi.org/assays/cystatin-c/>).
16. Brisco MA, Coca SG, Chen J, Owens AT, McCauley BD, Kimmel SE and Testani JM. Blood urea nitrogen/creatinine ratio identifies a high-risk but potentially reversible form of renal dysfunction in patients with decompensated heart failure. *Circulation Heart Fail*. 2013; 6:233-9.
17. Kidney Disease: Improving Global Outcomes (KDIGO) CKD Work Group. KDIGO 2012 Clinical Practice Guideline for the Evaluation and Management of Chronic Kidney Disease. *Kidney Int Suppl* 2013; 1-150.
18. Yu H, Yanagisawa Y, Forbes MA, Cooper EH, Crockson RA and MacLennan IC. Alpha-1-microglobulin: an indicator protein for renal tubular function. *J Clin Pathol*. 1983; 36:253-9.
19. Kohler H, Wandel E and Brunck B. Acanthocyturia--a characteristic marker for glomerular bleeding. *Kidney Int*. 1991; 40:115-20.
20. Wise GJ and Schlegel PN. Sterile pyuria. *New Engl J Med*. 2015;372:1048-54.
21. Kidney Disease: Improving Global Outcomes (KDIGO) Acute Kidney Injury Work Group. KDIGO Clinical Practice Guideline for Acute Kidney Injury. *Kidney Int Suppl*. 2012; 1-138.

22. Inker LA, Schmid CH, Tighiouart H, Eckfeldt JH, Feldman HI, Greene T, Kusek JW, Manzi J, Van Lente F, Zhang YL, Coresh J, Levey AS and Investigators C-E. Estimating glomerular filtration rate from serum creatinine and cystatin C. *New Engl J Med*. 2012; 367:20-9.
23. Levey AS, Stevens LA, Schmid CH, Zhang YL, Castro AF, 3rd, Feldman HI, Kusek JW, Eggers P, Van Lente F, Greene T, Coresh J and CKD EPI. A new equation to estimate glomerular filtration rate. *Ann Int Med*. 2009; 150:604-12.
24. Mullens W, Abrahams Z, Skouri HN, Francis GS, Taylor DO, Starling RC, Paganini E and Tang WH. Elevated intra-abdominal pressure in acute decompensated heart failure: a potential contributor to worsening renal function? *J Am Coll Cardiol*. 2008; 51:300-6.
25. Levey AS, Stevens LA, Schmid CH, Zhang YL, Castro AF, 3rd, Feldman HI, Kusek JW, Eggers P, Van Lente F, Greene T, Coresh J and CKD EPI. A new equation to estimate glomerular filtration rate. *Ann Int Med*. 2009; 150:604-12.